Biomicrofluidics REVIEW scitation.org/journal/bmf

Low-cost and cleanroom-free prototyping of microfluidic and electrochemical biosensors: Techniques in fabrication and bioconjugation

Cite as: Biomicrofluidics **15**, 061502 (2021); doi: 10.1063/5.0071176
Submitted: 13 September 2021 · Accepted: 22 October 2021 ·
Published Online: 8 November 2021

Mohd Afiq Mohd Asri,[1] Anis Nurashikin Nordin,[1,a)] and Nabilah Ramli[2]

AFFILIATIONS

[1]Department of Electrical and Computer Engineering, Kulliyyah of Engineering, International Islamic University Malaysia, 53100 Gombak, Selangor, Malaysia
[2]Department of Mechanical Engineering, Kulliyyah of Engineering, International Islamic University Malaysia, 53100 Gombak, Selangor, Malaysia

[a)]**Author to whom correspondence should be addressed:** anisnn@iium.edu.my

ABSTRACT

Integrated microfluidic biosensors enable powerful microscale analyses in biology, physics, and chemistry. However, conventional methods for fabrication of biosensors are dependent on cleanroom-based approaches requiring facilities that are expensive and are limited in access. This is especially prohibitive toward researchers in low- and middle-income countries. In this topical review, we introduce a selection of state-of-the-art, low-cost prototyping approaches of microfluidics devices and miniature sensor electronics for the fabrication of sensor devices, with focus on electrochemical biosensors. Approaches explored include xurography, cleanroom-free soft lithography, paper analytical devices, screen-printing, inkjet printing, and direct ink writing. Also reviewed are selected surface modification strategies for bio-conjugates, as well as examples of applications of low-cost microfabrication in biosensors. We also highlight several factors for consideration when selecting microfabrication methods appropriate for a project. Finally, we share our outlook on the impact of these low-cost prototyping strategies on research and development. Our goal for this review is to provide a starting point for researchers seeking to explore microfluidics and biosensors with lower entry barriers and smaller starting investment, especially ones from low resource settings.

I. INTRODUCTION

The development of microdevices such as lab-on-a-chip or μTAS is conventionally dependent on semiconductor microfabrication technologies, of which cleanroom facilities are central. Frugal prototyping of microdevices (also known as cleanroom-free microfabrication or desktop-compatible microfabrication and will be used interchangeably in this review) is the approach of using alternative techniques to produce some aspects of microfabrication achievable through cleanroom-based microfabrication, within the context of facilities, tools, and materials of lower cost and/or higher accessibility. Walsh and colleagues wrote a key editorial on moving microfluidics work from cleanroom to makerspaces, which briefly covers some alternative techniques but also highlighting important considerations in three main aspects of cleanroom-free microfabrication: design considerations (e.g., material compatibility with processing and application, fluidic connections), fabrication considerations (e.g., resolution), and assembly consideration (e.g., cleanliness, handling, alignment, bonding).[1]

The drive toward frugal prototyping stems from the reality that conventional microfabrication platforms, which often require either cleanroom (i.e., semiconductor fabrication) facilities or expensive industrial-grade pieces of machinery are not always available to academic or research institutions with low resources. For institutions without cleanroom facilities, often the available option for access is through rental and/or annual subscription to external cleanrooms. Furthermore, depending on the size of the device, often a single batch makes no more than a dozen units, limiting fabrication to low-volume manufacturing only. With every design and design iteration, a fresh process is required, thus accumulating the costs for a project. Costs aside, cleanroom facilities specialized for semiconductor and research applications are also limited in

low- and middle-income countries, especially, the ones that lack a robust semiconductor industry. Even in countries with existing electronics industry, it is often difficult for academic researchers to gain access to cleanrooms either due to logistical complexities (due to geographic distribution) or bureaucratic barriers. These financial and accessibility limitations led to the development of several new approaches toward microfabrication in microfluidics, electronics, and/or hybrid microdevices. Some approaches include 3D printing approaches[2] and the use of laminated films.[3] Some of these techniques can be completely independent of cleanrooms, while some others are partially dependent on cleanroom equipment, often in a context that eliminates the necessity of cleanroom facilities. More advanced techniques drove costs down to a few cents per unit device, and even use tools made commercially available for hobbyists and small businesses.

Our working definition for "low-cost approaches" in this review is methods that do not require specialized facilities such as cleanrooms and/or industrial-grade machineries (e.g., material deposition printer, injection molding machines, and robotic microarray spotter). In this review, we explore several approaches to low-cost and cleanroom-free prototyping for microfluidics devices and microelectrodes at the microscale/mesoscale. Descriptions of conventional methods for their microfabrication are provided at the beginning of each section, followed by descriptions of the low-cost methods. Methods included in this review incorporate low-cost strategies using commercially available desktop tools such as 3D printers, electronic craft cutters, laser engravers, and CNC micromilling machines. These tools are the most appropriate and accessible for under-resourced researchers. A short section on bioconjugation strategy compatible with low-cost devices is also included. Additionally, examples of integration microfluidics and electronics are presented. A focus on electrochemical biosensors is prevalent among the examples, as electrochemical biosensors are the most common form of integrated microfluidic–microelectrode devices amongst low-cost and cleanroom-independent prototyping methods.

A. Microfluidics and microelectrodes in biosensors

Biosensors are analytical devices incorporating biological elements as its sensing mechanism. The earliest work that introduced the definition of biosensors was by Leyland Clark in the 1960s, which described the electrochemical detection of oxygen or hydrogen peroxide as the basis of bioanalysis, by the incorporation of immobilized corresponding enzymes on electrodes.[4,5] Within the next two decades, biosensor development was exponential, with notable commercial successes in glucose meters for diabetic monitoring and home pregnancy test kits. Conventionally, bioanalyses are performed either through extensive wet lab protocols such as microbial culture, enzyme-linked immunosorbent assay (ELISA), and Western blotting;[6] through methods that require highly trained interpreters such as microscopy; or through methods requiring large instrumentation such as MALDI-TOF mass spectrometry,[7] high performance liquid chromatography,[8] or gene sequencing.[9] The miniaturization of bioanalysis through the technology that is now known as "lab-on-a-chip" (LoC) or "micro-total analytical systems" (μTAS) has enabled the decentralization of bioanalysis from central laboratories into clinical and field settings, with many of these LoC/μTAS devices utilizing biosensor concepts.[10] Modern applications of biosensors are many, including in biomedicine,[11–14] agriculture,[15–17] defence,[18] food quality control,[19,20] manufacturing of pharmaceuticals,[21,22] and fundamental sciences.[23,24]

Biosensors are diverse but one usually consists of two important components: its biorecognition elements and its signal transduction mechanism. Accordingly, they can be categorized according to either. The biorecognition element, or capture probes that are tethered to the surface of the biosensor, can be further categorized into: immunoproteins, enzymes, nucleic acids, and cell-based sensors. Some emerging categories of biorecognition include aptamers and molecular imprinted polymers.[25] Biosensors are also separated based on how signals from biological or chemical events are transduced and interpreted. The primary categories are optical (including fluorescence, transmissibility, reflectometry, and colorimetric assays), electrical and electrochemical (amperometric, voltammetric, impedimetric, and coulometric), electromechanical (including piezoelectric, acoustic waves, magnetic field, Hall effect, and gravimetric), and thermal (including thermoelectric).[10,26]

Two broad categories of innovations that has propelled the development of advanced biosensors and lab-on-a-chip devices are miniaturized electrodes and microfluidics. Microelectrodes, defined as electrodes with submillimeter dimensions,[27] when combined with microfluidics, enable superior mass transport capabilities such as large total surface area-to-volume ratio, large diffusion length to characteristic length ratio, and rapid steady-state responses[27] relative to macroelectrodes. Microfluidic–microelectrode integration also enables special fluid handling capabilities such as electrokinetic fluid manipulation.[28] Electrical and electrochemical sensors particularly benefit from the integration of these technologies.[26,29] A significant portion of this review will focus on works related to electrochemical biosensors.

1. Electrochemical biosensors

Commercially, electrochemical biosensors lead the biosensor market worldwide, particularly, in metabolite monitoring assays such as blood glucose monitoring.[5] Cost-wise, electrochemical biosensors represent the middle-ground between device costs and instrumentation costs: electrochemical sensors are often cheaper to make than electromechanical sensors, and the instrumentation it requires usually costs less than optical biosensors. Enzymes are often used as redox reporters in these biosensors, either directly in the case of biocatalytic biosensors, or conjugated to antigens or antibody in immunoaffinity biosensors.[30] Some examples of use cases of electrochemical biosensors include immunosensor for tuberculosis,[31] immunosensor for thyroid stimulating hormone,[32] and DNA sensor for *Ganoderma* sp., an oil palm pathogen.[15] Electrochemical biosensors are electrolytic cells, i.e., such that electrical energy is supplied into the system to drive chemical reactions, in contrast to the reverse, i.e., galvanic cells.[33] There are several considerations when designing an electrochemical biosensor, among them the selection of electrode materials. For biosensors, the working and counter electrode is often selected from inert materials that do not oxidize or reduce easily, such as gold, glassy carbon, or platinum.[34] For miniaturized biosensor, often a

pseudo-reference electrode is used, in which the reference electrode is in direct contact with the analyte solution without frit and electrolyte. The use of pseudo-reference electrodes in miniaturized sensors are often due to the limitations of its small form factor and/or the fabrication process of the sensor. Pseudo-reference electrode materials are chosen from those that have a stable equilibrium potential, such as silver–silver chloride, platinized platinum, or palladium–hydrogen.[35,36]

Developments in electrodes for electrochemistry has evolved over time from mercury drop electrodes to solid state macroelectrodes, to thick film and thin film electrodes.[37] Solid state electrodes for electrochemistry come in 2D and 3D forms. The miniaturization of electrodes into microelectrodes (sub-mm features) and ultramicroelectrodes (sub-100 μm features) has enhanced the capabilities of electrochemical sensing, due to its low ohmic drop, high diffusion length to characteristic length ratio, high faradaic to capacitive current ratios, rapid achievement of steady-state currents, and small volume samples. The low ohmic drop removes the requirement of supporting electrolytes, which may introduce contaminants in real sample analysis. We invite readers to this review by Daniele and Bragato for detailed analysis of advantages of microelectrodes in electroanalysis.[27] Among the different types of electrodes, solid-state planar electrodes are especially compatibility with printing technologies. Printing technologies enable low-cost and scalable design and manufacturing of miniaturized electrodes. Planar electrodes are also easier to integrate into microfluidic modules.

The evolution and convergence of mature technologies such as digital printing, photolithography for semiconductor electronics, and printed circuit boards have facilitated the emergence of new technologies for deposition of functional materials over wide substrates and the fabrication of printed sensors and electronics.[38] In recent years, flexible and stretchable electronics have been developed at an unprecedented rate and are involved in various applications, including sensors, displays, solar cells, supercapacitors, electronic skins, and wearable electronics.[39] Printed electrodes can be fabricated onto flexible substrates through mature technologies initially developed for semiconductors, such as physical vapor deposition; printing technologies, such as screen-printing, inkjet printing, and roll-to-roll printing; and bottom-up approaches, such as polymer assisted deposition and ion-exchange deposition.[39]

Advances in printed electronics fabrication techniques have led to rising application in mass-manufactured biosensors. In many configurations of biosensors, printed electrodes are common transducers that convert molecular events into an interpretable signal. Printed electrodes are used especially widely in electrochemical analysis[40,41] but is also used in other biosensing techniques such as impedimetric sensing,[42] surface acoustic wave spectroscopy (electromechanical sensing),[43] and surface-enhanced Raman spectroscopy (optical sensing).[44] Surfaces of sensors are often modified with functional materials to enable specific detection of analytical targets. Various printed electrodes for electrochemical sensing are now commercially available, which allow sensor research and development efforts being directed toward other sensing elements, such as molecular recognition layers and signal enhancement. Additionally, the advancement of microfluidics-integrated biosensors further contributed to the miniaturization of printed electrodes.[45]

2. Microfluidic biosensors

A major impact of miniaturization of biosensors is its integration to microfluidics technologies, which synergistically introduce new capabilities, such as parallelization and improved precision. Microfluidics, the manipulation and analysis of fluids at the microscale, is a powerful emerging technology and is currently being used for many applications in biology, chemistry, energy, defense, and pharmaceuticals. Its use is particularly popular in point-of-care testing (POCT) format due to miniaturization of assays and biosensors, which enabled them to fulfill the World Health Organization's recommended ASSURED (affordable, sensitive, specific, user-friendly, rapid, and robust, equipment-free, deliverable to end users) criteria for point-of-care diagnostics.[46]

There are various modalities of microfluidics devices, such as continuous flow microfluidics, droplet microfluidics, digital microfluidics, paperfluidics, and centrifugal microfluidics—each with their own advantages and limitations compared to the others. Additionally, there are many advantages to integrating biosensors from multiple high-throughput lab machineries into a microfluidic platform. Chen and Shamsi have written a comprehensive review on microfluidic biosensing.[10] In brief, the advantages of integrating microfluidics into biosensing platforms are primarily categorized into logistically related and reaction related. Logistically related advantages include lower sample and reagent consumption, lower material costs, and portability achieved through miniaturization. Reaction related advantages involve capabilities achieved through miniaturization on a single platform such as integrated multi-step protocols and parallelization, i.e., multiplexing of biochemical reactions, as well as special physicochemical effects of operating at the microscale, including: laminar flow, rapid diffusion, enhanced heat transfer, and heightened effects of electrical fields enabling electrokinetic manipulation and high-efficiency electrophoretic separation.[47] Several examples that take advantage of these effects include multiplexed biosensing of multiple targets in the same sample,[13] simulating physiological response in a blood vessel,[48] diffusion-based particle filtration across two buffers,[49] ultrafast electrophoretic separation,[50] ultrafast Western blotting for proteomic analysis,[51] and ultrafast heating and cooling for PCR.[52] Presently, various portable readout instruments are available, both commercially and as research-only tools, that is compatible with microfluidic flow cells designed for biosensing applications in various sensing modalities, including portable QCM readers,[53] potentiostats,[54] and optical sensors.[55]

While electrochemical biosensors and microfluidic biosensors each has its own merits independent of each other, the integration of both types of analytical devices creates a synergistic relationship that empowers each other's inherent features.[26,37] As previously described, introducing microfluidics into electrochemical sensors provides portability, enables additional sample preparation capabilities, improves its mass transport, and lowers its resource consumption. Conversely, electrochemical sensors are especially suitable for integration into microfluidic analytical devices due to it being the least limited by cost and size factors in device miniaturization and scaled-up manufacturing, relative to other modes of sensing.[37]

II. APPROACHES TO PROTOTYPING MICROFLUIDIC DEVICES

A. Methods using photolithography and industrial machineries

The majority of LOC are made using cleanroom-associated technologies, which was first developed for the fabrication of semiconductor devices such as diodes, transistors, and integrated circuits, and later adopted by the micro-electromechanical systems (MEMS) in the 1980s that produces accelerometers, miniature pressure, and temperature sensors and GPS integrated devices.[56] Among cleanroom-associated equipment are photolithographic mask aligners and thin film deposition machines, such as metal sputtering chambers and plasma-enhanced chemical vapor deposition. The earliest works of microfluidic MEMS utilized etched silicon or glass substrates. Silicon was widely used in the beginning primarily due to familiarity with the material and the processes involved from integrated circuit processes, while glass is used extensively in devices made for biological purposes, as most of the biochemical reactions have been characterized in glass.[57] Later works focus more on polymers, as they are easier to machine.

A major driver toward the exponential development of fluidic circuits is the introduction of a technique called *soft lithography*. In soft lithography, microstructured patterns are formed onto polydimethylsiloxane (PDMS) elastomer using patterned molds. The technique was first introduced by Xia and Whitesides in 1998 using photolithographed SU-8 resist master molds.[58] Deriving from this work, more recent works in recent years often use alternative approaches for master molds for soft lithography, such as using polished 3D-printed molds,[59,60] micromilled thermoplastic molds,[61] or dry film resists.[62] PDMS became a popular material of choice in biological applications due to its optical transparency, its gas permeability and water impermeability, its chemical inertness and non-toxicity to cells, and its ease of processing due to easy casting of its precursors and a plasma-activatable surface.[63]

However, soft lithography's approach that requires casting polymers precursors into molds was limited in mass manufacturing as the processing time cycle per batch takes too long (due to polymer curing time and demolding process) for it to be manufacturable at high volumes. Researchers then resort to *injection molding* and *hot embossing*, two techniques widely applied in production of plastic items such as toys and household utensils. In micro-injection molding, melted thermoplastic is poured into micromachined molds and then cooled under the thermoplastic's glass transition temperature.[64] Hot embossing involved pressing thermoplastic blocks, sheets, or pellets between heated master molds to form the intended shapes.[65] The master molds for both techniques can be fabricated using standard micromachining processes, as in the case of silicon masters, or using high precision milling techniques such as electrical discharge machining (EDM) in the case of steel masters.

As fabrication technologies develop, one emerging technique in the fabrication of polymer-based microfluidic devices is through *stereolithographic 3D printing*, where microfluidic devices are directly fabricated through curable resin, eliminating the need for molds. A further advanced approach is photopolymer inkjet printing, which forms structures similar to fused deposition modeling, but has the resolution of resin-based stereolithography. Albert Folch and colleagues wrote a comprehensive review on 3D printing approach in microfluidic device fabrication.[2] Additionally, *multi-material printing* enables additional versatility for biosensor printing beyond the typical polymer-based materials, adding sacrificial materials (such as sugars and other water-soluble materials) and bio-based inks (often cells or tissues carried in hydrogels) as printable options.[66]

B. Low-cost and desktop-compatible methods

Despite its versatility, cleanrooms are not necessarily easy to access, especially to researchers in low- and middle-income (LMIC) countries, and the facilities and equipment involved are expensive.[1,67] Similarly, while Dimatix printers are more affordable than cleanrooms, it is still cost-prohibitive to acquire and maintain to many researchers in low-resource settings. These associated costs and access barriers hinder prototyping through iterative design process, delays product delivery, and discourages lab-on-chip development and applications in low- and middle-income countries (LMIC). To overcome these financial and access barriers, several independent works has been developed to build sensors and microfluidic devices to various degrees of limitations in geometric resolution, material versatility, and complexity. The prototyping methods described in this section is categorized based on its primary structural material: paper, PDMS resin (soft lithography), sheet thermoplastics, and glass.

1. Paper-based microfluidics

Paper-based microfluidics, also known as paperfluidics and micro-paper analytical devices (μPAD), was also pioneered by the Whitesides group in 2007, which drew inspiration from lateral flow assay (LFA) devices such as home pregnancy test kits.[68] Relying on principles of capillary wicking in paper substrates, μPAD utilizes hydrophobic and hydrophilic patterning on paper to develop microchannels within the paper itself. This can be achieved not only using the conventional photolithography and resist-based plasma treatment but also with various alternative techniques including wax printing, flexographic printing, and paper cutting.[69]

Some of the reasons that μPAD is very attractive for μTAS devices is the low cost, ease of scale, and disposability of paper substrates. Paper is very cheap at the mass manufacturing scale, and many mass-production models have been developed with paper in other industries such as newspaper printing, publishing, tissue papers, and filters. It is also biodegradable and non-toxic when incinerated, which is an attractive feature for disposable devices that involves hazardous wastes. It also comes with a particular commercial tool that increases its accessibility to most developers in the world, the Xerox ColorQube and its corresponding proprietary Solid Ink technology, which allows high-resolution wax printing be acquired and performed at low cost.[70] Xerox, however, recently discontinued the product line in late 2018, which may cause the accessibility to this technique to wane in the future. One other low-cost alternative toward creating hydrophobic barriers in paper is using correction pens (white-outs), although this method sacrifices resolution and precision.[71]

Paper, however, has several limitations as fluidic and electronics materials, which has hindered its adoption in μTAS devices. μPAD typically has a relatively high limit of detection (LOD), which limits its sensitivity as an analytical device. Paper patterning techniques such as wax printing typically have lower resolution compared to non-paper techniques (in the ~300 μm range at its highest resolution), and the requirement of having the hydrophobic ink to be embedded inside the substrate instead of on the surface further reduces its spatial resolution. Additionally, the inherent nature of paper causes difficulty to introduce valving and timing controls on a device, which limits its programmability as a time-controlled, multiple step analytical device, and often necessitates manual intervention from operators. Regardless, μPAD has been successfully deployed as analytical tools.[72]

Building on earlier μPAD works, the Yager group at University of Washington pioneered the development in two-dimensional paperfluidic networks (2DPNs). The two-dimensional network strategy improves on the 1-dimensional μPAD and LFAs by introducing valving and timing features onto a paperfluidic device[73] [Fig. 1(a)]. This has enabled programmability of multi-step reactions onto the device, which minimizes the human intervention steps during an analytical process. Additionally, they have added washing steps and reagent-based signal amplification on the 2DPN platform, which improves on the LOD of the device to be on par with the analytical level of standard laboratory enzyme-linked immunosorbent assay (ELISA), which they demonstrated through a portable malaria sensor.[74]

Within the context of electrochemical microfluidic biosensors, Ataide *et al.* has compiled an excellent review regarding a decade of development of electrochemical paper-based analytical devices[75] that merges the fluid control in paperfluidic devices with electronic printing on paper substrates. Several noteworthy examples were highlighted, including a pop-up paperfluidic biosensor that enables flow timing and functionality switching by folding[76] and a 16-channel multiplexed electrochemical biosensor.[77]

2. Low-cost soft lithography

Building upon soft lithography, but without expensive facilities to process photoresists, several alternative approaches for making mold masters have been developed. *Vinyl sticker*-based molds can be cut easily using commercial plotter-cutters. Additionally, *UV nail polish* has been used as a low-cost photoresist that is usable with a photomask made from high-resolution laser printer.[78] Once the master has been made, PDMS device is made as per standard soft lithography. A comparative study between soft lithography device made using vinyl sticker vs UV nail polish molds has been performed, with UV nail polish considered the superior option in precision and resolution.[79] Other rapid approach for making a mold master include dry resist films.[80]

The *Embedded SCAffold RemovinG Open Technology* (ESCARGOT) technique was first introduced in 2015, as an improved method to soft lithography[81] [Fig. 1(b)]. ESCARGOT leverages on the solvability of acrylonitrile butadiene styrene (ABS), a common thermoplastic used in 3D printers, in acetone. ESCARGOT works by immersing an ABS mold inside a pre-cured PDMS, curing the PDMS, and then dissolving the ABS mold in acetone. This enables a completely enclosed microchannel formation inside the PDMS structure that does not require bonding steps. It also allows three-dimensional microchannel structures inside the PDMS, as well as embedding electronic components prior to PDMS curing. An additional benefit of this technique is the fact that PDMS, ABS, and acetone are all low cost and easily accessible materials, and commercial 3D printers are increasingly getting cheaper. A significant limitation to ESCARGOT relative to other methods described in this review is it is a relatively slow fabrication technique, as mold dissolution can take from few hours to several days depending on the size of the mold, and the dissolving rate of the mold–solvent pair. Additionally, there are not many combinations of substrate–mold–solvent that are available besides PDMS–ABS–acetone, as these are largely unexplored. One approach is heat-dissolved 3D-printed wax molds, however, the heat requirement may affect other steps in multi-process fabrication.[82] A recent 2018 study found that 3D-printed *o*-toluenesulfonamide and *p*-ethylbenzenesulfonamide copolymer mold dissolves faster in acetone without damaging PDMS, which is an improvement to the ESCARGOT method.[83] The ESCARGOT method always creates a closed microfluidic channel, which may create difficulties in region-specific patterning of chemical and biological functionalities onto the inner surfaces of the channels, which is simpler to perform on open-channel configurations. This can be resolved through photopolymeric functionalization, although this introduces some additional steps onto the fabrication process.[84]

3. Low-cost microfabrication in sheet thermoplastics

Thermoplastics such as polystyrene, polyethylene terephthalate (PET), polyvinyl chloride (PVC), polymethyl methacrylate (PMMA), polycarbonate, cyclic olefin copolymers (COC), and polyimide are commodity materials that are cheap and easily available in sheet form of various sizes and thicknesses worldwide. Machining microdevices using sheet thermoplastics as a starting substrate allows prototyping without the need of custom molds such as used in injection molding.

Michelle Khine's group at University of California Irvine pioneered the use of *Shrinky-Dinks* as a rapid, low-cost, cleanroom-free technique for microfluidic prototyping, both as a mold for soft lithography[85] and as a structural material[86] [Fig. 1(c)]. Shrinky-Dinks is a children's toy made from biaxially-oriented polystyrene thermoplastic, in which the 2D film shrinks when it is heated and forms a 3D shape. Drawn, printed, or etched patterns on the film are embossed in its shrunk form, making it suitable for mold-making. Shrinky-Dinks microfluidics have been used for applications such as stem cell culture[87] and cellular biomechanical studies.[88]

The earliest approaches to bypassing soft lithography and injection molding for prototyping and moving toward benchtop-based fabrication, is the application of *xurography*, i.e., pattern cutting of polymer sheets using a plotter-cutter machine and laminating the 2D layers to form 3D structures[89–91] [Fig. 1(e)]. Polymer sheets such as polyethylene terephthalate (PET, commercially sold as Mylar), polyimide (commercially sold as Kapton), or poly methyl methacrylate (PMMA/acrylic) are low-cost and widely available commodity. Rapid development of such work has been accelerated by commercialization of home-use plotter-cutter tools

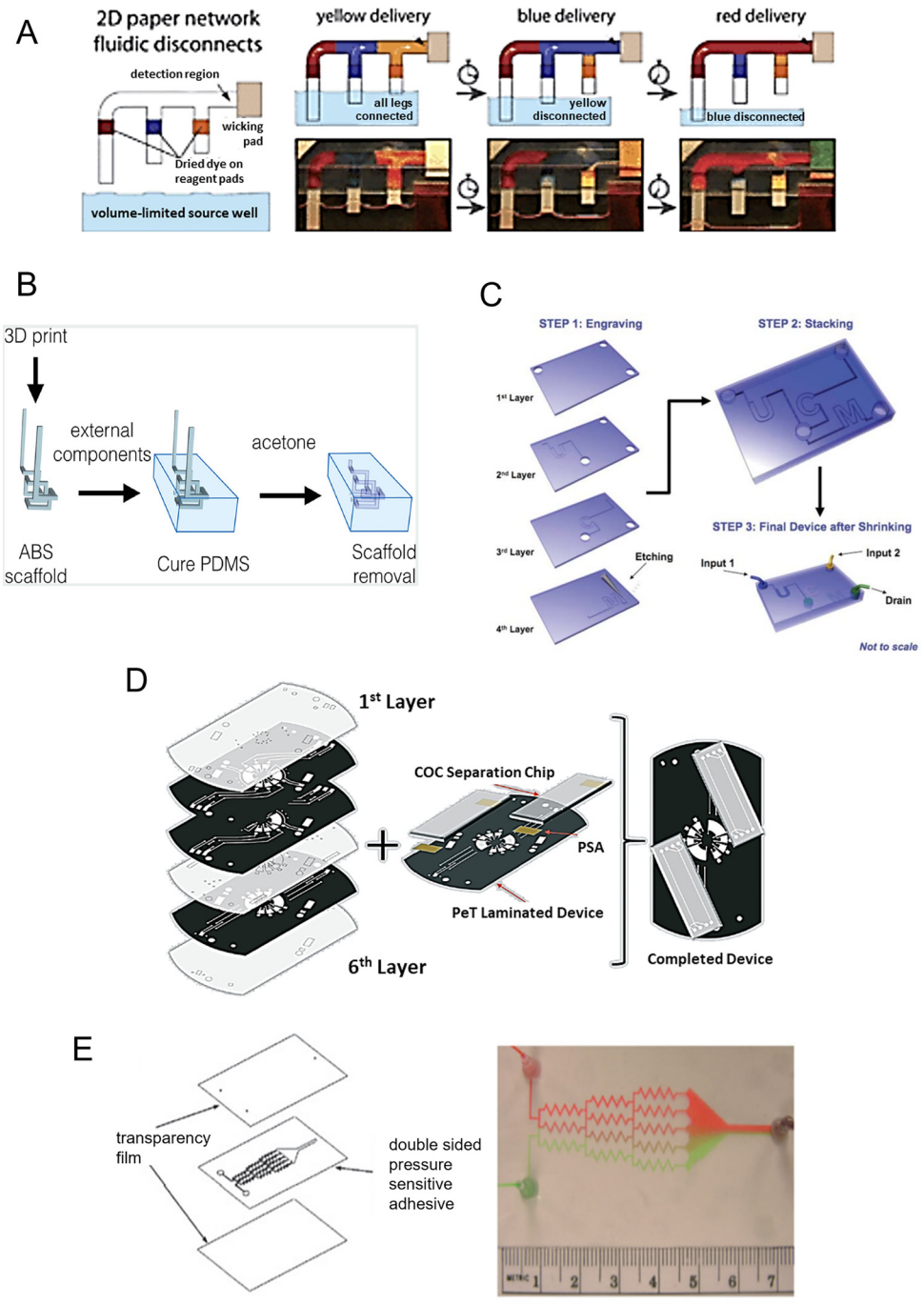

FIG. 1. Selected illustrations of low-cost fabrication processes for microfluidic devices. (a) Two-dimensional paperfluidic network. Image reproduced with permission from Lutz *et al.*, Lab Chip **11**, 4274 (2011). Copyright 2011 the Royal Society of Chemistry. (b) Process flow for preparation of microfluidic device using the ESCARGOT method, reproduced from Saggiomo and Velders, Adv. Sci. **2**, 1500125 (2015), Author(s) licensed under a Creative Commons Attribution (CC BY 4.0) license. (c) Step-by-step process for fabrication of the microfluidic device from the engraved Shrinky-Dinks film. Image reproduced with permission from Chen *et al.*., Lab Chip **8**, 622 (2008). Copyright 2008 the Royal Society of Chemistry. (d) Concept of a print-cut-laminate device with integrated gold leaf. The black colored layers are printed with toners on both sides. Image reproduced with permission from Thompson *et al.*, Lab Chip **16**, 4569 (2016). Copyright 2016 the Royal Society of Chemistry. (e) Concept and example of a microfluidic device made by xurography of transparency films and pressure-sensitive adhesives, reproduced with permission from Yuen and Goral, Lab Chip **10**, 384 (2010). Copyright 2010 the Royal Society of Chemistry.

such as the Silhouette Cameo® and the Cricut Air™. Such an approach of cut-and-laminate microdevice prototyping is well-summarized in this lab-on-a-foil review by Focke *et al.*[3]

A derivative work of the laminated foil technique, the *print-cut-laminate* (PCL) technique was first published by the Landers group in *Nature Protocols* in 2015.[92] This technique takes advantage of the adhesive property of the styrene acrylate or styrene butadiene polymers in laser-jet printer toners when it is melted and then cooled. PCL is achieved through the following: (1) polyethylene terephthalate (PET) films are laser-printed on both sides to form a heat-activated adhesive surface, (2) microchannels are patterned on the PET film using laser cutters or cutting plotters, and (3) the layers of patterned PET sheets are bonded together using an office laminator. This method enables a very rapid, low-cost method to build μTAS devices, both in consumables and instrumentation. Other lamination strategies has also been explored, such as using pressure-sensitive adhesive and heat-sensitive adhesive, as well as using metal foils as a laminated substrate layer.[93,94] Overall, the design-to-product process of a single prototyping iteration with PCL takes around 2 h. Limitations of PCL are that toner printing only permits flexible and printable substrate materials, cutting plotters and laminators can work with only thin substrates, as well as the low burst pressure of toner as adhesive. These issues are later circumvented using pressure- and heat-sensitive adhesives, and in 2017, the Landers group successfully built a fully-integrated DNA profiling platform for forensics application using this fabrication method[95] [Fig. 1(d)]. Laser cutters increase the costs of equipment compared to cutting plotters, however, is still significantly cheaper than cleanroom techniques.

While xurography is convenient for plastic film and paper-based materials, it is not workable with thicker and more rigid materials such as poly methyl methacrylate (PMMA/acrylic) or cyclic olefin copolymer (COC) sheets. *Laser cutting* or CNC milling is often used for such materials instead. Laser cutting acrylic or COC sheets has been used to make microfluidic devices in combination with other materials[96] or as engraved microchannels within the same sheet.[97] For laser-cut thermoplastic devices, Klunder *et al.* introduced a simple device sealing approach exploiting the melting temperature difference between polycaprolactone and PMMA.[97] The popularity of *CNC micromilling* as a microdevice fabrication tool is emerging as desktop CNC milling tools became cheaper and more accessible. Lashkaripour *et al.* characterized micromilling strategies and optimized parameters to build microfluidic devices using a desktop CNC milling tool and was able to achieve microchannel resolution of 75 μm in polycarbonate.[98] This approach is generally expandable to most sheet thermoplastics. Additionally, Liu *et al.* overcame the inherently high surface roughness of CNC micromilled microfluidic channels by coating the channels with PDMS pre-polymer and gas-blowing the microchannels.[99] This approach creates microchannels with smooth, non-rigid, and biocompatible walls and enables elliptical channel cross section. While the tools are relatively more expensive than plotter-cutter, laser cutters, or CNC milling machines are more robust and covers a more versatile selection of workable materials, with exceptions of transparent or reflective materials unsuitable for IR laser cutters, and soft and stretchy substrates (such as textiles) not suitable for CNC milling.

4. Low-cost microfabrication on glass

While most low-cost approaches focus on polymer or thermoplastics as the workable material, several approaches focused on low-cost micromachining on glass substrates. Glass is optically transparent, which can be important depending on the microfluidic application. It can also be easily procured, often in the glass slide form. Micromachining in glass require care as the substrate is brittle.

Ku and colleagues extended the use of CNC micromilling to soda-lime glass slides.[100] They found that microchannels can be milled into glass substrates without fracturing when milling is performed while the glass is immersed in water with optimized spindle rotation of 8000 rpm at slow feed rates (< 500 μm/min). This works was able to achieve microchannel resolution of 100 μm in glass. However, the channel height is limited to 100 μm to avoid fracturing.

The use of *Armour Etch*, a hobbyist glass etching paste containing ammonium biflouride, is used together with vinyl sticker stencils to form microchannels on glass substrates.[101] The team reports an etch rate of 5 μm depth per hour. While this technique presents the simplest approach for chemical etching of glass devices, it is acknowledged that the etching rate is slower and does not etch as cleanly as hydrofluoric acid due to under-etching, which causes high surface roughness. Caution and extreme care are required when using Armour Etch as it can also penetrate through the skin and cause deep tissue damage, although to a less potent extent than hydrofluoric acid.

The low-cost microfluidic prototyping approaches presented above are summarized in Figure 1 and Table I. Tabulated summary may include additional information not discussed in the main text.

III. APPROACHES TO PROTOTYPING PRINTED ELECTRONICS

A. Conventional thin film fabrication and PCB manufacturing

Patterning of electrically conducting materials is necessary in the development of semiconductor chips and electrical circuits. Recent developments in materials and techniques used for printed electronics allows for advanced applications such as flexible displays, photovoltaics, chemical sensors, and bioelectrodes.

Conventionally, semiconductor microelectronics (and more recently, nanoelectronics), especially CMOS transistors and silicon MEMS devices, are developed using *thin film technologies*. Briefly, the process involve (1) preparation of a mask (usually chromium), (2) coating of substrate with photoresist, (3) transferring the mask pattern onto the photoresist using a mask aligner, (4) developing the resist, (5) depositing a thin film of conductor or dielectric (often by sputtering) or removing a material through dry or wet etching, and (6) removing the resist. This cycle is repeated for each layer until the device is formed, and individual units are diced. These processes are often performed in cleanrooms - facilities with controlled laminar air flow to reduce particulate matter that can affect thin film formation. These processes of UV photolithography, bulk micromachining, and surface micromachining have been covered in depth in Refs. 47 and, 102. A conventional thin film

TABLE I. Summary of low-cost techniques for the fabrication of microfluidic devices.

Technique	Tools necessary	Features	Strengths	Limitations
Paper-based microfluidics	Laser-cutter,[73,74] ColorQube wax printer and hot plate[70]	· Detection limit 2.9 ng/ml, assay time 30 mins[74] 1 mm wax channel resolution[70]	· Extremely low cost per device Easily disposable and is biodegradable	• Low sensitivity, require amplification strategy
• Difficult to program analytical steps				
Soft lithography by low-cost molds (vinyl stickers, UV nail polish, Shrinky-Dinks)	Cutting plotter,[79] UV lamp,[78] toaster oven[85]	· Vinyl sticker: minimum linewidth 200 μm (straight), 500 μm (curved), height min 80 μm		
· Nail polish: minimum linewidth 100 μm, max depth 1 mm				
· Shrinky-Dinks: minimum linewidth 65 μm, depths 50–80 μm	· Extremely low cost per device			
· Utilizes low-cost tools	• Limited resolution compared to photoresists			
• PDMS devices may still need plasma oven for bonding				
Soft lithography using dry resist films[80]	UV lamp and laminator	• 5 μm minimum thickness		
• Minimum linewidth 10 μm, 20 μm gaps	• Near nanometer resolution, as good as cleanroom photoresist methods but cheaper and simpler steps	• PDMS devices may still need plasma oven for bonding		
• Films of non-standard thicknesses are more expensive				
Micromilled thermoplastic[98]	CNC milling machine	• Resolution: features 75 μm, gap 250 μm		
• Fabrication time < 1 h				
• Fabrication cost < USD6.00	• Workable materials are cheap and easily accessible			
• Able to machine 2D and 3D features on plastic and glass	• High end micromilling machines are expensive			
• Does not work with stretchable materials				
Etched Shrinky-Dinks[86]	Toaster oven	• Minimum channel width 8 μm		
• Depth: 50–600 μm	• Can achieve very small microchannels			
• Does not require special tools for parts bonding	• Process requires optimization to control device dimensions post-shrinking			
Print-cut-laminate[92,95]	Laser printer, laser cutter and laminator	• Minimum channel width 100 μm		
• Fabrication time ~ 40 min	• Rapid prototyping of multilayered devices			
• Can easily integrate with electronic parts and surface modifications	• Toner-based devices have low burst pressure			

TABLE I. (*Continued.*)

Technique	Tools necessary	Features	Strengths	Limitations
• Laser cutter and heat-sensitive adhesive are pricy				
Xurography and laminated thermoplastics[90,91]	Cutting plotter and laminator	• Minimum line width 100 μm (polyimide), 250 μm (PET)		
• Fabrication time ~ 15 min	• Rapid prototyping of multilayered devices			
• Easily accessible equipment and materials				
• Can easily integrate with electronic parts and surface modifications	• Restricted to thin substrates			
• Resolution is dependent on type of substrate				
ESCARGOT[81]	FDM 3D printer	• Resolution: 100 μm		
• Fabrication time: 12 h or more	• Quickly fabricate closed channels			
• Enables 3D features	• Long dissolving time			
• Limits use of surface modifications requiring open channels				
• Limited workable material combinations				
Armour Etch microfluidics[101]	Cutting plotter	• Minimum linewidth 250 μm		
• Depth < 5 μm				
• Etching time ~4 h	• Enables low-cost micromachining on glass	• High surface roughness due to uneven isotropic etching		

process is also used for preparing nanoimprint lithography stamps, which is used in the fabrication of flexible electronics through roll-to-roll processes.[103]

Another conventional approach is the manufacturing of *printed circuit boards* (PCBs), which often consists of copper layer (conductive material) on FR4 fiberglass substrate (dielectric) and often coated with a resin as solder mask.[104] This combination is most optimal for standard soldering of electronic components. For flexible printed electronics, the most common substrate is polyimide due to its high heat tolerance. PCBs can be single layer or multilayered, with its copper layer being single-sided or double-sided, and the different layers of copper can be connected to each other through vertical interconnect access (via) holes. Like microelectronics, PCBs are also patterned using photolithography, although its processing is often limited to wet etching to subtract materials, while metal layers are added through electroplating instead of sputtering. PCBs are widely used in hardware of industrial and consumer electronics, and service manufacturers are available globally for made-to-order custom designs. Various computer aided design (CAD) softwares for designing PCBs are also widely available.

PCB is also considered a low-cost approach toward microelectrode manufacturing and are often fabricated in-house for various research applications, especially ones where bare copper electrodes are required. Low-cost rapid patterning of PCBs can be performed using CNC micromilling[105] or toner-transfer lithographic process.[106] Some examples of use of PCBs in biosensor fabrication include in digital microfluidic biosensors[107] and electrochemical sensors.[108]

B. Conductive ink-based printing

The scalability of production of printed electronics has been made easier due to the development of conductive inks, and later its commercialization to the mass market. Carbon-based ink can be made at-home using graphite, although better quality inks have been made available commercially for hobbyists and educators, such as Bare Conductive paints. Silver ink is made by incorporating silver powder or flakes into a binding agent, such as Circuit Scribe that caters conductive silver ink pens to hobbyist and educators. Inks for home consumer use are often water-soluble. Niche manufacturers such as Gwent produce high performance metal ink

products, including gold, silver, carbon, and copper pastes made for industrial and academic use.

The most well-established ink-based technique is *screen-printing* and *stencil printing*. Screen-printing has been used traditionally in art, textiles, and publishing. Within μTAS devices, the screen-printing is the most successful fabrication technique that does not require cleanrooms, owing to the success of mass-manufactured home glucose measurement kits.[5] Briefly, screen-printing involves patterning and deposition of ink - typically viscous paste or a gel, onto a substrate through a mesh stencil called a silkscreen[109] [Fig. 2(a)]. The ink is pressed through the silkscreen using a squeegee tool to deposit a thin layer of ink onto the substrate. Stencil printing uses similar masking approach, however, removes the mesh from the stencils, which makes the stencil easier to prepare but limits control over uniformity of electrode thicknesses. Screen-printed electrodes are particularly successful commercially, its scalability have given rise to several disposable electrode brands, most notably DropSens, which their products have been widely used for R&D of several electrochemical and/or biosensors.[12,110,111]

The strength of screen-printing is the wide variety of inks and substrates available of which screen-printing can be applied. Various functional inks has been developed, such as metal pastes, e.g., gold, silver, platinum, and carbon; resists and wax; as well as conductive polymers such as poly(3,4-ethylenedioxythiophene) polystyrene sulfonate (PEDOT:PSS)[112] or polyaniline (PANI).[113] Screen-printing works on various substrates, including glass, silicon, paper, fiberglass, and textiles. This technique has been used to develop electrochemical sensors,[114] surface acoustic wave sensors,[115] and quartz crystal microbalances.[116] Screen-printing also enables low-cost and rapid mass manufacturing of devices due to its ability to fabricate multiple devices in parallel. The main limitation of screen-printing is its need for customized silkscreen, which lengthens the time taken between design iterations during prototyping phase. In this sense, screen-printing involves the same turnaround time as cleanroom-associated photolithography techniques, which requires customized photomasks.

Next to screen-printing, *inkjet printing* (IJP) is the most explored alternative fabrication technology. Recent advances in inkjet printing technologies—particularly, high dot per inch piezoelectric print-heads, has opened doors to various IJP deposition methods involving various types of inks and substrates.[117] The most used IJP equipment is the Dimatix-2800 series multi-material inkjet printer. While it costs in the hundreds of thousands of dollars, the Dimatix printer is versatile, able to print various types of ink including colloidal metals, liquid polymers, and biologicals. It can also work with various types of substrates - rigid ones such as glass and FR4 boards, flexible ones such as Kapton films and PET, as well as elastomers such as cured PDMS. Some of the micro-devices that has been developed through Dimatix-based IJP include functional electronic transistors,[118] biological patterning,[119] and sensor-integrated multilayered microfluidic device.[120]

To further drive costs down, systems that can work with commercial office inkjet printers are developed. The most widely commercialized product is colloidal silver nanoparticles (AgNP) in aqueous solution as ink[121] [Fig. 2(c)]. This low-cost IJP method has been utilized for several μTAS devices. Dixon *et al.*[122] used AgNP ink in off-the-shelf inkjet printers to fabricate functional electrowetting-on-dielectric (EWOD) microfluidic devices that has demonstrated to run rubella immunoassay, and Kawahara *et al.*[16] used commercial IJP to fabricate soil and leaf humidity sensors for agricultural purposes. As inkjet printing is a quick process, typically consuming between 1 and 3 min, the iterative turnaround time with IJP techniques is especially short. Ink consumption is also typically low, thus significantly reducing cost. The main limitation for consumer-grade IJP platforms is that they have very limited number of inks available for them, and the substrate type is restricted to thin and flexible materials such as paper and PET films. While restricting the system to only silver metal electrodes and paper and PET substrates, commercial printer IJP fabrication has better spatial resolution, higher repeatability, maskless process, and fast fabrication speed.[117,123] As for research-grade IJP platforms, the drawback is its high equipment cost, which may be prohibitive for lesser-funded groups; as well as its necessity to optimize print settings such as ink formulations and ink deposition speed to enable reproducible fabrication process. Inks used for IJP requires its Ohsenorge number, which relates the density, viscosity, and surface tension of the fluid to the diameter of the nozzle to be between 0.02 and 1.5 to be able to print out optimally.[124]

Another approach of patterning conductive ink is through a method called *direct ink writing (DIW)*. DIW is, in principle, similar to IJP, however, it utilizes larger nozzles that are smaller in number (usually single-nozzled) and can function with custom-made or commercial conductive ink without requiring very low ink viscosities. One example of using DIW for electrode sensors is the fabrication of carbon nanotubes and silver nanoparticle electrochemical electrodes onto photopaper substrate, by pairing a digital plotter (Cricut Air™) with a ballpoint pen filled with the conductive inks[125] [Fig. 2(d)]. Choi Keun-Ho and colleagues at UNIST fabricated a hand-drawn Zn-air battery on paper using CircuitScribe silver conductive pen, graphite from an 8B pencil, and a custom ink from zinc nanoparticles and linseed oil mixture carried in a ballpoint pen.[126] An advantage of DIW is it is easier to maintain as it less likely for the ink carrier (e.g., pen, single-nozzle extruders) to clog and is cheaper to replace if it is broken. DIW also provides fast prototyping such as IJP as it does not require mask preparation like screen-printing. However, for low-cost tools, DIW suffers from poor resolution, often ranging only from the mesoscale to milliscale.

C. Novel approaches to microelectrode fabrication

Besides conventional methods and ink-based prototyping of printed electronics, several other techniques have been developed for various merits. One such reason is cost efficiency at low production scale, as the previous techniques can be prohibitively costly without mass production. Another reason is compatibility with substrate materials or with process integration. This section will exhibit some examples of these non-conventional approaches.

1. Laser-induced graphene

An emerging strategy to produce conductive traces cheaply and rapidly is using laser-induced graphene made from polyimide precursors. A discovery by Rice University researchers, first

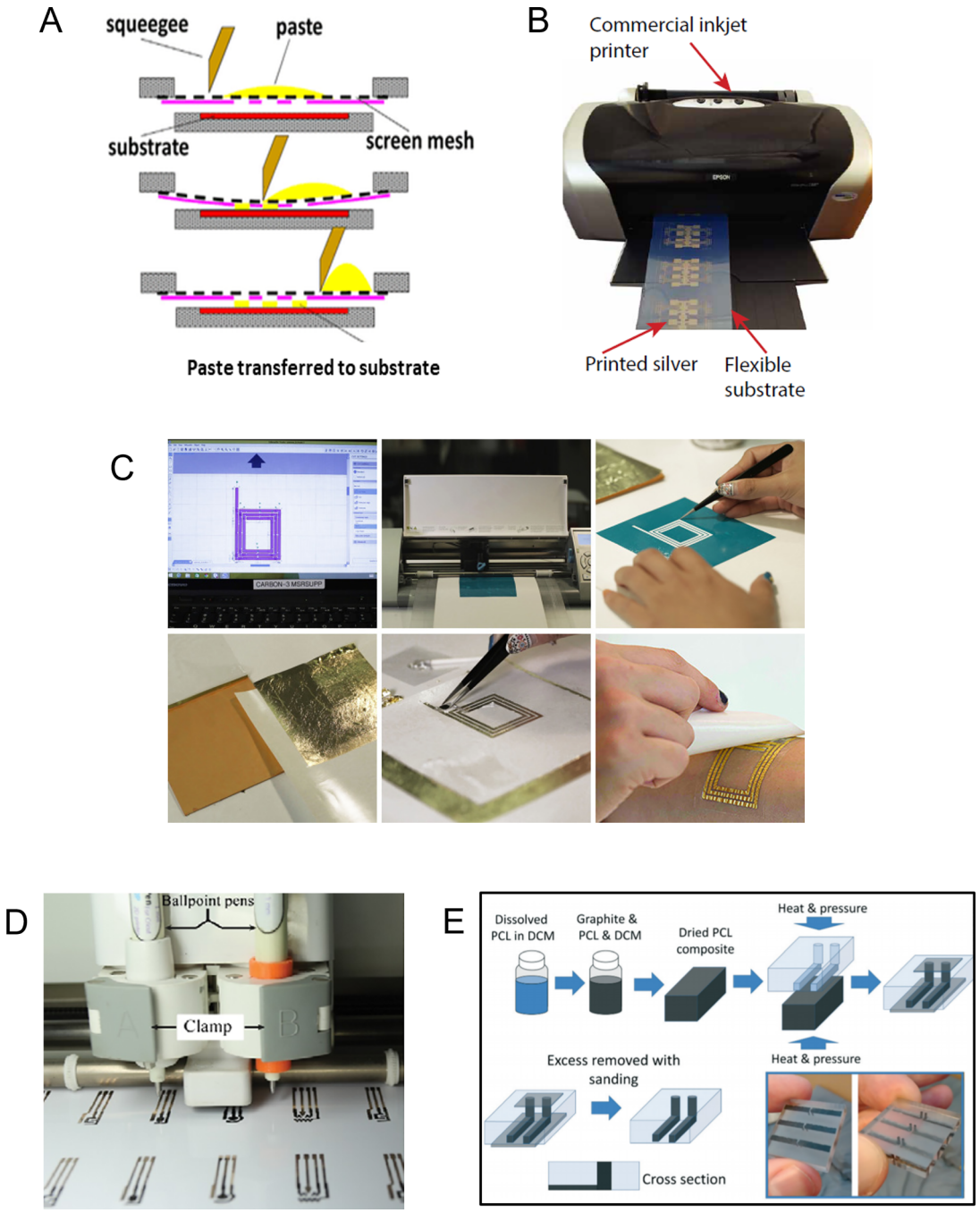

FIG. 2. Selected illustrations of low-cost printed electronics devices, with focus on unconventional techniques. (a) Steps for screen-printing conductive ink onto a substrate, image reproduced with permission from Kudr *et al.*, Sens. Actuators, B **246**, 578 (2017). Copyright Elsevier, 2017. (b) Step-by-step process for fabrication of DuoSkin,[132] an electronic skin with patterned electrode made from gold leaf. Photo by Cindy Kao, MS Media and MIT Media Lab, retrieved from cindykao.com/DuoSkin. Copyright 2015. Author(s), licensed under a Creative Commons—Attribution-Non Commercial-Share Alike 4.0 International (CC BY-NC-SA 4.0) License.[143] (c) Printing of electrode array on flexible substrate using silver nanoparticle ink loaded on a commercial inkjet printer. Image reproduced with permission from Dixon *et al.*, Lab Chip **16**, 4560 (2016). Copyright 2016 the Royal Society of Chemistry. (d) Direct ink writing of conductive ink using ballpoint pens and electronic plotter. Image reproduced from Soum *et al.*, ACS Omega **3**, 16866 (2018). Copyright 2018 Author(s) ACS Author Choice license.[125] (e) Electrodes from graphite-embedded polycaprolactone, press-molded into laser-engraved thermoplastic templates. Image reproduced with permission from Klunder *et al.*, Lab Chip **19**, 2589 (2019). Copyright 2019 the Royal Society of Chemistry.

published in 2014, discovered that commercially available polyimide substrates such as Kapton can used as precursor substrate to be converted into 3D porous graphene films using commercial CO_2 infrared laser engravers.[127] The same study demonstrated its application in microsupercapacitors. This technique provides a rapid and facile approach to fabrication of graphene-derived electrodes, including reduced graphene oxides (rGO). This method is also favored due to the resultant graphene's large surface area for molecular immobilization.[128,129] This approach have been applied for the fabrication of wearable biosensors.[130,131] Amorphous graphene made using this approach has excellent surface properties, however, exhibit high impedance and lower conductivity compared to metal-based electrical traces.

2. Gold leaf

Kao *et al.* utilized vinyl stickers as temporary stencils on the substrate to pattern gold leaf electrodes for electronic skin fabrication, which is an effective technique to fabricate microstructured gold leaf electrodes *in situ* down to 0.5 mm in the feature size[132] [Fig. 2(b)]. This work has been demonstrated for use as the capacitive human–computer interface. However, limitations arise when adapting this method into electrochemical sensors as the vinyl stenciling produces jagged electrode edges, which affects uniformity of current distribution. Furthermore, the method involves stacking of gold leaf to overcome gold leaf ruptures due to mechanical stress from the stenciling process, which, in turn, increases electrode impedance due to the dielectric adhesives in between the gold leaves. Works by Landers group at University of Virginia utilized laser-cut gold leaves laminated onto polyethylene terephthalate (PET) and poly-methylmethacrylate (PMMA) sheets to rapidly build a DNA electrophoresis platform[94] and has recently demonstrated its ability to prepare samples for forensic DNA profiling.[95] Santos *et al.* are among the first to use gold leaf sandwiched between Kapton tapes as nanobandgap electrodes for electrochemical use,[133] with its exposed surface area to analyte limited to the z-axis thickness of the gold leaf (usually in hundreds of nanometers). Additionally, Wang *et al.* integrated gold leaf onto polyester fabric to form wearable supercapacitors, and then polypyrrole nanorods are electrodeposited.[134]

3. Metallic foils

Works involving non-gold leaf metal foils as electrodes include use of aluminum foil as spark gap electrodes in a low-cost cell electroporation platform[135] and use of CO_2 and fiber laser cutting on copper foil to form high frequency circuits on Kapton tapes.[136] An instant printed circuit board film, Printem, utilized pre-deposited UV photoresist to pattern copper foil.[137] The film is designed such that the patterning can be performed using printer toner as UV mask, and the etch/development is performed immediately by selective foil removal through differential adhesion. Mohammadzadeh *et al.* presents a clever approach to pattern copper at high resolution as part of an integrated electro-microfluidics platform. UV-curable dicing tape is taped onto copper foil and geometries are cut using commercial cutting plotter. The dicing tape is then cured by UV to create permanent adhesion to the copper foil and unwanted regions can then be peeled away easily.[138] This approach enables electrode widths as small as 66 μm. In the context of electrochemistry, copper and aluminum are, however, not inert, which presents a limitation when working with oxidizing species in the fluid. Copper substrate is also not biocompatible in applications requiring cell culture in microdevices.[139]

4. Liquid metal

For making circuits for highly stretchable substrates, using liquid metal is more suitable than solid, sintered conductive ink. Liquid metal conforms to the shape of its container and does not cause electrical discontinuity due to cracking as the substrate is flexed or stretched. For example, gallium–indium–tin alloy (Galinstan) is liquid at room temperature and can be contained within microchannels in a stretchable substrate such as Ecoflex.[140] An example of commercially available Galinstan is Thermal Grizzly's Conductonaut. However, as the conducting material is liquid, its sensing modalities cannot interact directly with an analyte, thus limiting it to capacitive or strain-based sensing.

5. Carbon-derived pastes

Klunder *et al.* merges its conductive material into the substrate: graphite powder were mixed into dichloromethane-dissolved polycaprolactone (PCL) pellets, and later press-molded the carbon–PCL mixture into an electrode template made by laser engraving onto an acrylic sheet[97] [Fig. 2(e)]. This method is low-cost and enables a simple parts bonding process, which is crucial for assembly of an integrated microfluidic biosensor. McIntyre *et al.* applies the same principle of milling the electrode template, filling it with carbon paste, and sealing it with adhesive tape and has demonstrated its capability in capacitive droplet sensing and sorting.[141] The latter work used Bare Conductive carbon ink, which is cheap, commercially available, water soluble, and easy to handle and dispose as compared to Klunder *et al.*'s work involving dichloromethane. The drawback of a water-soluble ink is it could not be used in applications where the electrodes interfaces directly with fluids.

The low-cost printed electronics approaches presented above are summarized in Fig. 2 and Table II. Tabulated summary may include additional information not discussed in the main text.

IV. SURFACE CONJUGATION OF BIO-AFFINITY MOLECULES ONTO ELECTRODES

A primary feature in most biosensors, regardless of sensing mode (electrochemical, optical, and electromechanical) is the localized immobilization of biomolecules or chemistry onto the sensing region of the device. These molecules may react specifically with the analyte of interest within the bulk sample. This section covers some of the approaches to immobilize these molecules, with focus on surface-based chemistry. We refer readers to Kim and Herr's review for a more comprehensive bioconjugation techniques for proteins;[145] however, here we will discuss techniques compatible with low-cost electrodes. The selected techniques here also do not require costly specialized instrumentation such as microarray spotters and are not dependent on conjugation strategies requiring

TABLE II. Summary of low-cost techniques for the fabrication of printed electronics.

Approach	Type of conductive ink	Features	Strengths	Limitations
Screen-printing[109,114]	Silver, gold, carbon, silver chloride, graphene, PEDOT:PSS, PANI	• Resolution: 200 μm trace, 200 μm gaps		
• Z-thickness: 16 μm	• Rapid device production at mass manufacturing scale			
• Relatively large variety of paste and substrate	• Require custom silkscreen			
• slow turnaround time between iteration				
Dimatix inkjet printing[109,117,118]	Silver, gold, carbon, silver chloride, graphene, carbon nanotubes, PEDOT:PSS, PANI	• Resolution: 100 μm trace		
• Gap: 30 μm				
• Z-thickness: 2 μm	• Highly versatile, workable with various inks and substrates	• Dimatix DMP2800 printer is costly		
• Require process optimization for each type of ink				
Commercial inkjet printing[16,122]	Silver	• Resolution: 100 μm trace, 100 μm gaps,[122] 250 μm trace[121]		
• Z-thickness: 300 nm				
• Sheet resistance: 0.19 Ω/sq	• Printer is cheap and easily accessible			
• Printing process is only a few seconds	• Limited to only silver inks			
• Limited to PET and paper substrates				
Direct ink writing[125,144]	Silver, carbon, nickel	• Resolution: 225 μm trace, 140 μm gaps		
• Z-thickness: 300 nm				
• Unit device cost: USD0.014	• Easily integrable with cutting plotter			
• Cheap and easy to maintain	• Limited variety of ink			
• Resolution is limited to size of pen tip				
Laser-induced graphene[127,131]	Porous graphene	• Resolution: 100 μm trace		
• Z-thickness: 25 μm				
• Sheet resistance: 15 Ω/sq	• Maskless process, single-step fabrication			
• Raw material is easily available				
• Rapid fabrication of graphene	• High sheet resistance compared to metallic electrodes			
Gold leaf, laser cut[94,95]	Gold	• Resolution: 2 mm		
• Unit cost per electrode: USD0.10	• Integrable with laminated sensor/microfluidics devices	• Only allow simple, milliscale geometry		
• Process requires caution as gold leaf is fragile				
Gold leaf, DuoSkin[132]	Gold	• Resolution: 0.5 mm trace		
• Z-thickness < 150 nm				
• Unit device cost (with NFC electronics): USD2.50	• Integrable with laminated sensor devices			
• Allows for complex geometry	• Process requires caution as gold leaf is fragile			
• Electrode edges are jagged				
Copper foils, tape[136]	Copper	• Resolution: 0.5 mm trace		
• Cyclic flexing test: robust until 2000 cycles	• Highly conductive, can carry high frequency signals			

TABLE II. (*Continued.*)

Approach	Type of conductive ink	Features	Strengths	Limitations
• Able to fabricate multilayer VIAs	• Copper not suitable for biological interfacing			
Copper foils, UV-curable patterning and xurography[138]	Copper	• Resolution: 66 μm trace, 25 μm gaps		
• Fabrication time: < 30 min	• Simple fabrication of fine electrical traces			
• Integrable with laminated sensor/ microfluidics devices				
• Highly conductive, can carry high frequency signals	• Copper not suitable for biological interfacing, requires electroplating			
Liquid metals[140]	Galium–indium–tin (Galinstan)	• Conductivity: 0.01–0.02 Ω/sq		
• Maximum strain: 450%				
• Trace width: 0.5 mm				
• Fabrication time: ∼1 h	• Conducts electricity without hysteresis in stretchable devices	• Requires microfluidic channels to carry conductive element		
• Not suitable for direct contact of conductive materials to bio-analytes				
Press-molded polycarbonate–graphite composite[97]	Carbon	• Conductivity: 200 S/m		
• Bonding temperature: 85 °C	• Easily integrable with microfluidic elements			
• Simple plastic-to-plastic bonding	• Carbon not very conductive			
• Process involve hazardous solvent				
Templated Bare Conductive electrode[141]	Carbon	• Resolution: 75 μm		
• Electrode depth: 50 μm				
• Resistivity: 0.28 Ω cm	• Ink and substrates are cheap and easily accessible			
• Easily integrable with microfluidic elements				
• Tools are commercially available				
• Simple sealing method	• Electrode not interfaceable with fluid samples			
• Carbon has high impedance, not suitable for high frequency signals				

physical or chemical vapor deposition,[146,147] which typically are performed in cleanroom environments.

A. Conjugation chemistry for biomolecules on electrodes

The simplest approach to attach biomolecules to a surface is through *adsorption*. Adsorption, or physisorption, is the non-specific interaction of a biomolecule to solid surface and is affected by hydrophobicity, electrostatics, formation of hydrogen bonds, and van der Waals interactions.[148] Adsorption allows much simpler immobilization process compared to cross-linking, chemisorption, and entrapment. It is also the mildest surface immobilization approach, thus confer the greatest potential to preserve the native structure of the biorecognition element, especially, in the case of proteins where chemical modifications can potentially change its folding state. The major disadvantage of simple physisorption is that the biorecognition molecules can easily be displaced during washing steps during fabrication or desorb into the analyte solution during analysis due to competing biomolecules or change in pH.[149] Despite this, adsorption of biomolecules to a polymeric surface can be enhanced through plasma activation and heating of the polymer substrate near its glass transition temperature, where the protein conjugation is comparable to the attachment achievable using a EDC/NHS linker.[150]

Carbodiimide cross-linking is a popular approach to attach proteins onto a surface, one of the most popular carbodiimide compounds being (1-ethyl-3-(3-dimethylaminopropyl)carbodiimide or EDC. EDC specifically functions as an activator for forming an amide bond between carboxylic acids and primary

amines, the latter forms the backbone of proteins. EDC forms an active O-acylisourea intermediate that is easily displaced by nucleophilic attack from primary amino groups, forming an isourea by-product in the reaction mix. While the intermediate is unstable, often *N*-hydroxysuccinimide (NHS) or its water-soluble analog (Sulfo-NHS) is often added to EDC-coupling procedures to improve conjugation efficiency or create dry-stable, amine-reactive intermediates, as EDC/NHS reactions form a stable NHS ester that acts as placeholder for the incoming protein.[151] The use of EDC/NHS is dependent on the generation of carboxyl groups on the surface intended for conjugation, which can be achieved through surface activation in some materials, by polymeric grafting,[152] or through self-assembled monolayers[153] [Fig. 3(a)].

Similar to EDC/NHS, other chemisorption approaches that leverage on tail group moieties exist. *Glutaraldehyde cross-linking* is a method such that glutaraldehyde, a bifunctional reagent with two aldehyde groups, forms imine bonds between two amino groups (such as proteins) with itself. Effectively, glutaraldehyde cross-linking attaches two amine ($-NH_2$) moieties together, with a five-carbon chain in between.[154,155] Another interesting chemisorption approach is by *silane cross-linking*. Among silanizing agents often used are aminosilanes such as (3-aminopropyl)triethoxysilane (APTES) and epoxysilanes such as 3-glycidoxypropyltriethoxysilane (GPTES). It is known from silicone-based bonding (such as PDMS–PDMS bonding) that two surfaces with silanol ($-Si-OH$) moieties can be bonded together by hydrolysis to form siloxane ($Si-O-Si$) bonds. Silanes ($-Si-H_2$) can be oxidized into silanol through plasma activation. Silane cross-linking is useful for attaching proteins to silicone or to bond thermoplastics to silicone surfaces[156–158] [Fig. 3(b)].

One specific form of chemisorption that is particularly useful for protein conjugation to metals is *self-assembling monolayer* (SAM). SAM is the assembling of molecules through chemisorption of a chemical "head group" moiety onto a substrate surface, followed by spontaneous reorganization of the "tail group". Most notable practical examples of such phenomenon are thiols on metals[159,160] and siloxanes to oxide surfaces.[161] In biosensor fabrication, thiol SAMs are prevalent in the functionalization of proteins such as antigens, antibodies, and enzymes onto metal surfaces or metallic nanoparticles, by utilizing carboxyl tail groups coupled with EDC/NHS reaction to form amine bonding.[151]

Gold being one of the most common materials favored as electrochemical working electrodes due to its chemical inertness, low chemisorption property, wide double layer region,[162] and its electro-catalytic behaviour,[163] benefits from its ability to form Au-S bonds with thiolated molecules as self-assembling monolayers in appropriate conditions.[164,165] Gold-thiol has been extensively exploited for surface functionalization in gold thin films, thick films, and nanoparticles.[110,166] Asiaei *et al.* demonstrated that immersion in 10 mM thiol ethanolic solution generates a gold-thiol surface monolayer within 15 mins.[167] Some examples of gold-thiol SAM in biosensor probes include using 11-mercaptoundecanoic acid (11-MUA) to form gold-thiol SAM, and then conjugating antibodies to the acid tail using EDC/NHS chemistry[153] and polyethylene glycol linker with sulfur head group and biotinylated tail group to link streptavidin anchors onto gold surface, which is then used to capture biotinylated IgG antibodies.[168]

Another approach that is used for conjugation is through bioaffinity. Several protein–protein interactions in nature yields high binding constants (more commonly used to describe such interaction is the dissociation constant, K_D, in which the smaller value of K_D the stronger the binding), notably antigen–antibody interactions. More commonly used for surface conjugation purposes is the *biotin and streptavidin* pair. Streptavidin and biotin are proteins are extracted from bacteria *Streptomyces avidinii* and has the strongest known non-covalent binding between a protein and its ligand at the scale of $K_D \sim 10^{-15}$ M. Streptavidin-avidin bonds have been utilized for protein and nucleic acid attachments in many bioengineering applications due to its femtomolar affinity and protein stability against high temperature, organic solvents, and extreme pH.[169,170] Other types of bioaffinity conjugation include using *polyhistidine chains* to transition metal ions such as copper, cobalt, zinc, and nickel ions, embedded within a matrix.[171] A chain of six or more histidine amino acid residues engineered into the conjugate protein of interest can form a complex with the transition metal ions at $K_D \sim 10^{-13}$ M.

B. Integrating surface modification into fabrication process

While the previous section provides a window into commonly used chemistry for conjugating biomolecules to any surface, this section introduces several common processes for surface modification within the context of microdevice fabrication.

The simplest approach to introduce a surface modification onto a surface is by *drop casting*. In essence, drop casting is simply the process of leaving droplet of a solution containing the intended chemistry to react with the surface.[172] This reaction can be as simple as adsorption or a chemical modification of the substrate (i.e., chemisorption), or a reaction with a pre-existing moiety on the surface. Drop casting works only within processes where a surface is outwardly accessible to a liquid handling tool (e.g., pipettes, syringes) and does not work for modifying enclosed device surfaces, however, can be used to prime surfaces with selective chemistries prior to device bonding or enclosure, where other reactants can be introduced to the surface in later downstream processes through solution flow into the enclosed surface. Drop casting is particularly popular among works involving commercial screen-printed electrochemical sensors due to the SPEs inherent open-surface architecture and integration of electrochemistry in the modification process, i.e., deposition through electrosorption process.[12,111,173] Some examples of open-surface drop casting-based modification include introducing antibodies onto a quartz crystal microbalance using self-assembled monolayer and EDC–NHS chemistry,[153] while closed surface priming is demonstrated in Bruch *et al.* where a surface is modified with Teflon to introduce a hydrophobic stop barrier prior to microchannel sealing, which allows all subsequent surface modification to occur upstream the microchannel without affecting its downstream portion during device processing.[174] Drop casting can also be integrated into digital fabrication tools, such as a plotter where a custom bio-ink is loaded into a refillable technical pen to deposit programmable biomolecule pattern on a substrate,[144] or an inkjet printer to deposit colorimetric reagents as dried spots on PET substrate.[124]

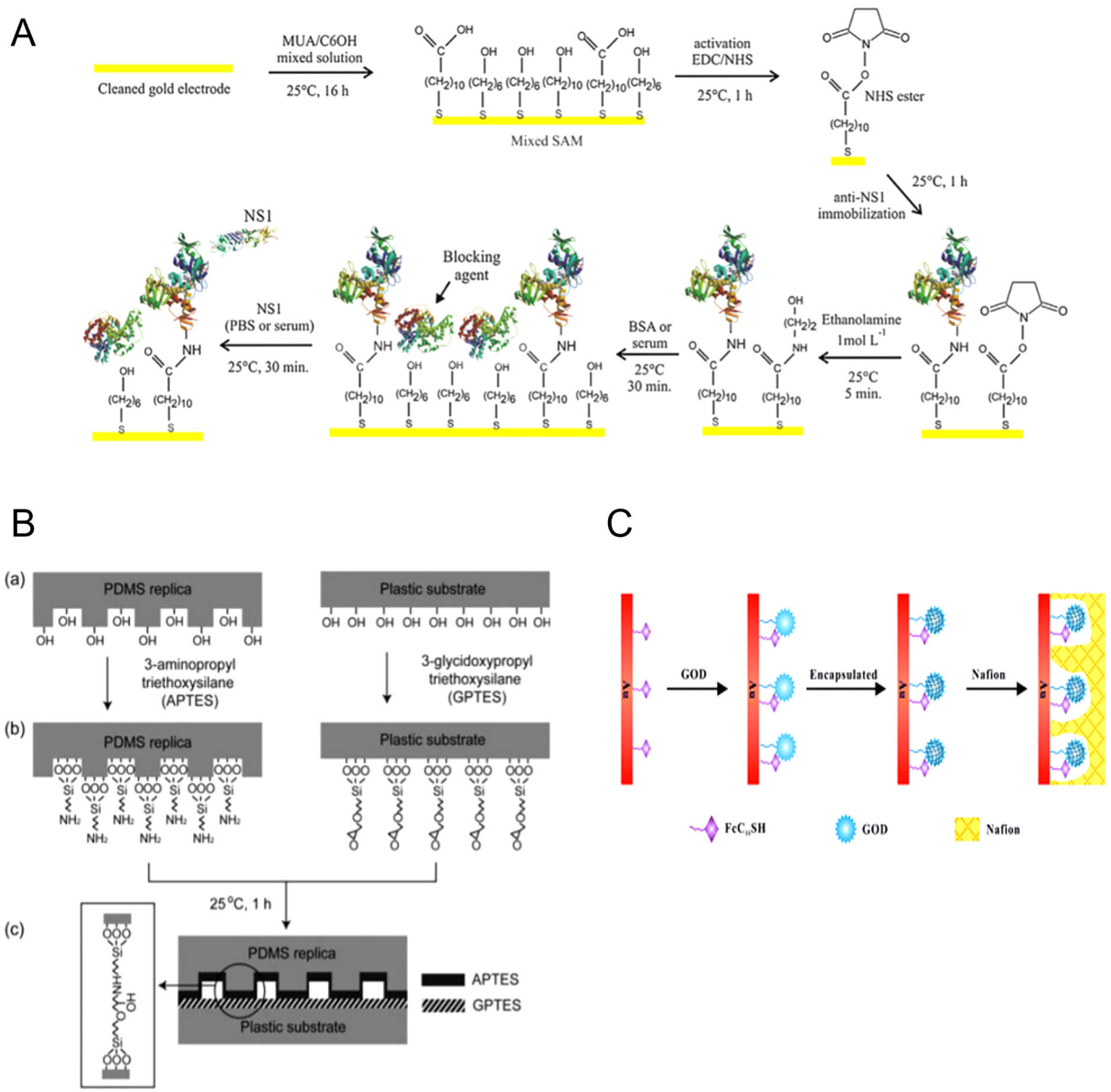

FIG. 3. Selected illustrations of conjugation strategies for immobilizing biomolecules onto biosensor surfaces. (a) Application of gold-thiol SAM and EDC–NHS bioconjugation, reproduced with permission from Cecchetto *et al.*, Sens. Actuators, B **213**, 150 (2015). Copyright Elsevier, 2015. (b) Chemistry of attachment of aminosilanes and epoxysilanes onto a surface with activated hydroxyl moieties, and application of bonding through hydrolysis. Image reproduced with permission from Tang and Lee, Lab Chip **10**, 1274 (2010). Copyright Royal Society of Chemistry, 2010. (c) Example of glucose oxidase (GOD) enzyme immobilization on the sensor surface through polymer encapsulation. Image reproduced with permission from Peng *et al.*, Analyst **136**, 4003 (2011). Copyright 2011 the Royal Society of Chemistry.

Another common approach to retain biologics on a sensor surface or a localized region within the device is by entrapping the biomolecules within a *gel or membrane matrix*. A frequently chosen membrane used for this application is Nafion, an ionic polymer which is highly selective in allowing flow of cation but not anions or electrons. One such example is the use of Nafion as the immobilizing matrix for glucose oxidase for enzymatic detection of glucose[175,176] [Fig. 3(c)]. Other forms of polymer matrix has also been used, for example, John Rogers' group at Northwestern used polyvinyl chloride–chitosan matrix as immobilizing and anti-leaching membrane for lactate oxidase enzyme and tetrathiafulvalene (redox mediator) in their sweat bioanalysis sensor.[177] The

membrane also acts to limit the concentration of analytes that contacts the electrode and prevents surface fouling. Additionally, hydrogels have also been used for localizing biological probes in a microfluidic biosensor, particularly larger-sized biologics such as live cells. Hydrogels are co-polymer matrices that allow flow of water in and out of its gel phase. Yeast cells (*Saccharomyces cerevisiae*) have been encapsulated in an alginate gel film lined along the microchannel of a high-efficiency ethanol bioreactor.[178] Eydelnant, Li, and Wheeler built spheroid cell culture bioreactors by mixing canine kidney cells into the sol phase (colloidal) of Geltrex extracellular matrix proteins, localized them solution in microfluidic device using premade hydrophilic sites, and thermally polymerizes them.[220] An advantage of using matrix-based immobilization is that often all the pre-polymer and biomolecules that make up the components of the matrix can be prepared in one solution and applied to the device with minimal steps. Some disadvantages of this approach compared to covalent bonding of biomolecular probes to the electrode surface is the longer distance of electron transfer (which may diminish signals) and that the gel phase is often three-dimensional (as opposed to surface-tethered biomolecules that can be treated as a two-dimensional element), which may introduce undesired impedance in fluid flow within a microfluidic device.

Within enclosed microchannels, one approach to locally modify the inaccessible inner surface is through *photopolymerization*. Localized regions within PDMS microchannels can be primed for attachment by UV-light photografting of polyacrylamide (PAAm) to the PDMS. Region-specific treatment is performed by masking the device using a photomask made on transparency film. A mixture of PAAm pre-polymer and benzophenone photoinitiator is flowed into the microchannel, and the masked device is irradiated using UV light. This creates a carboxylic acid moiety on the selected region, which primes the surface for EDC-coupling of proteins.[84] This approach requires the substrate to be optically transparent or translucent, which is effective given that PDMS is a common substrate in microfluidic devices made through soft lithography (or similarly derived approaches).

Figure 3 illustrates several mechanisms of surface chemistry from the selection of examples discussed in this section.

V. EXAMPLES OF DESKTOP-FABRICATED BIOSENSORS WITH INTEGRATED ELECTRONICS AND/OR MICROFLUIDICS

This section showcases examples of application of the techniques covered in Secs. II–IV. These examples often use many of the featured techniques in combination, however, also covers microdevices that are partially dependent on conventional approaches, and sensors that contains printed electronics and microfluidics but do not necessarily detect through electrochemical means. The last few examples cover methods that fully utilize desktop-compatible fabrication for electrochemical microfluidic biosensors.

A. Partially cleanroom-dependent electrochemical microfluidic biosensors

Kim and Shin *et al.* developed an electrochemical microfluidic immunoassay platform whereby the sample processing fluidic circuit was made of layered, laser-cut PET, acrylic sheets, and pressure-sensitive adhesives[179] [Fig. 4(a)]. This work demonstrates an early work in electrochemical microfluidic biosensing in which the fabrication process is minimally dependent on expensive instrumentation, except for its gold biosensing electrodes, which was fabricated via sputtering gold through a shadow mask. This platform was demonstrated for application in a four-step creatinine kinase-myocardial band (CK-MB) immunoassay, which yields a limit of detection of 0.25 ng ml^{-1}. Similar approach using milled polycarbonate sheets and pressure-sensitive adhesive paired with thin film electrochemical electrodes (platinum–platinum–silver) have also been used for multiplexed amperometric detection of the carcinoembryonic antigen (CEA) and cancer antigen 15-3 (CA15-3).[180,181]

Can Dincer's group at University of Freiburg, Germany rapidly prototyped electrochemical microfluidic biosensors using alternating layers of polyimide, dry resist films, and spin-coated photoresist. The platinum–platinum–silver chloride set of electrodes are made through photolithography and sputtering onto the polyimide substrate.[174] The device is demonstrated for detection of microRNA in serum, particularly, tumor biomarkers miRNA-19b and miRNA-20a, using CRISPR-Cas13a cleavage mechanism coupled with a competitive immunoassay.[182] The cleavage caused diminishing redox signal within the system, which is recorded amperometrically. The device achieved overall processing time of 4 h, readout time of 9 min, and a limit of detection of 10 pM using a measuring volume of less than 0.6 μl.

B. Desktop-compatible fabrication for non-electrochemical microfluidic biosensors

Dixon *et al.* at the University of Toronto used inkjet printing on commercial Epson C88+ printers used with Novacentrix's silver nanoparticle ink and substrates to print electrode arrays for digital microfluidic biosensors.[122] The electrodes are then coated with Cyanoresin cyanoethyl pullulan (CEP) dielectric and Fluoropel hydrophobic layer through roll-to-roll manufacturing. This approach achieved cleanroom-free fabrication at unit device cost of USD 0.63. The fabrication process was validated by building a 13-step rubella virus (RV) IgG immunoassay platform, which yielded a limit of detection of 0.02 IU ml^{-1}. The measurement was performed by chemiluminescence signals detectable through an optical sensor (photomultiplier tube).

Linnes group at Purdue developed a microfluidic isothermal nucleic acid amplification test for HIV in whole blood samples, with colorimetric-based sensing.[183] The microfluidic circuitry to perform blood sample cleanup consists of primarily nitrocellulose membranes and pre-deposited reagents laminated in plastics paired with a commercial dipstick HIV test for detection and quantifiable through a smartphone-based software. The flow timing is achieved through wax valving, which is actuated using reusable printed thermal resistors, made of silver ink printed on polyimide using a Dimatix platform. This work claims that the consumable components cost as low as USD 2.23 per assay with the reusable components costed at most USD 70 without mass production; and achieved an LOD of 2.3×10^7 virus copies per ml. This example is a microfluidic biosensor with integrated electronics, however, does not apply electrochemical sensing.

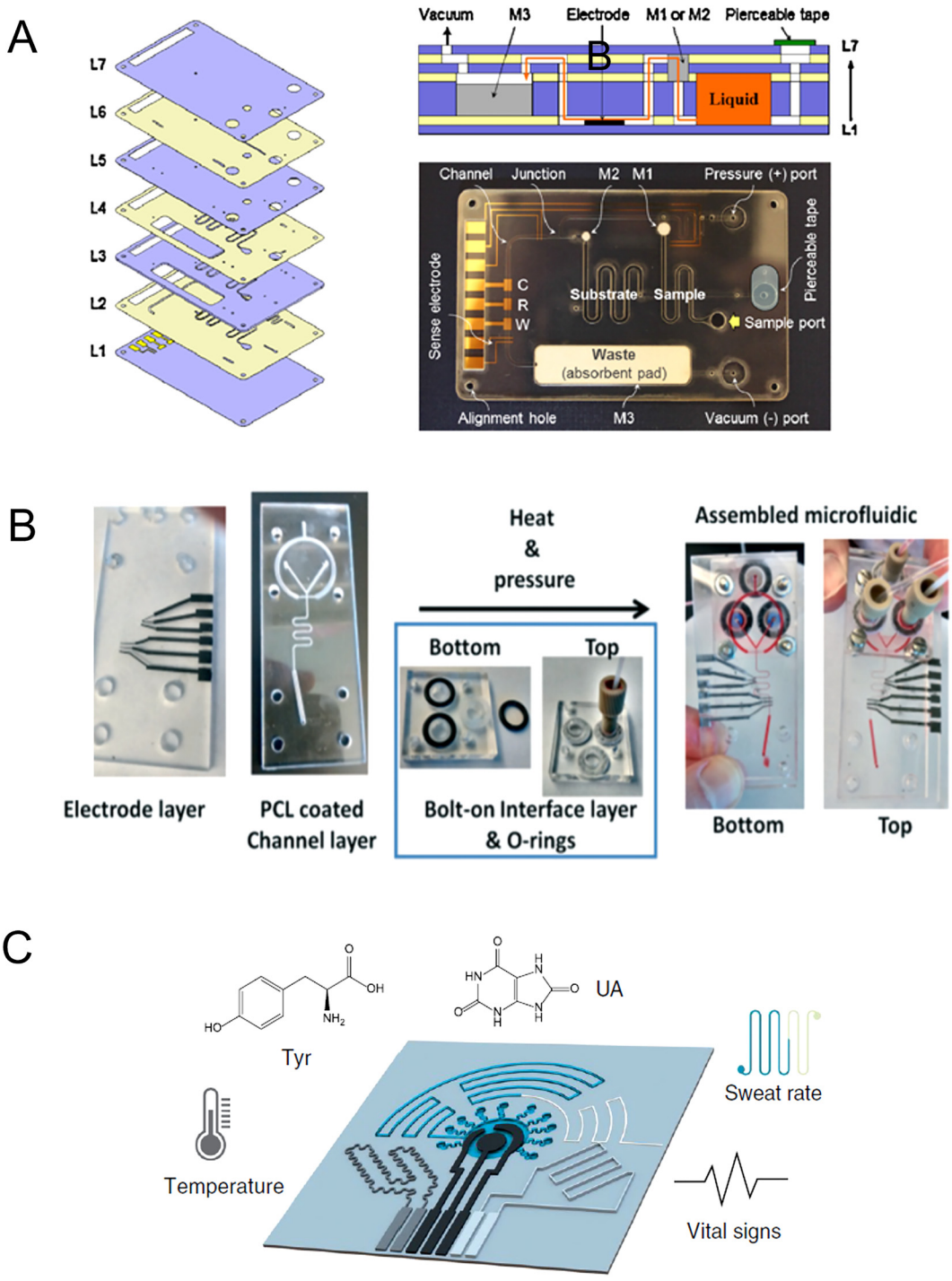

FIG. 4. (a) Electrochemical microfluidic biosensor for CK-MB immunoassay, fabricated with laminated thermoplastic and adhesives and sputtered gold electrodes. Image reproduced with permission from Kim *et al.*, Sens. Actuators, B **202**, 60 (2014). Copyright Elsevier, 2014. (b) Electrochemical organic synthesis platform using graphite–polycaprolactone electrodes embedded in a PMMA microfluidic chip. Image reproduced with permission from Klunder *et al.*, Lab Chip **19**, 2589 (2019). Copyright 2019 the Royal Society of Chemistry. (c) Wearable sweat sensor from integrated laser-induced graphene and laser-cut tape-based microfluidics. Image reproduced with permission from Yang *et al.*, Nat. Biotechnol. **38**, 217 (2020). Copyright Springer-Nature, 2020.

Landers group at University of Virginia pioneered the earliest microfluidic biosensor with gold leaf electrodes integrated into print-cut-laminate devices,[94] and later improved the workflow by integrating gold leaf electrodes into laminated PET-acrylic/COC-adhesive devices that resulted in a fully-microfluidic three-component kit for DNA extraction, PCR amplification and electrophoretic separation for applications in forensic DNA profiling.[95] The latter work improved the prior work by increasing its robustness against delamination (centrifugal speed up to 3000 rpm), high temperatures (up to 105 °C), and high voltages (200–1800 V). The electrophoresed DNA is then profiled and achieved resolution as high as 2 base pairs within separation distance as short as 40 mm, with 100% match to benchmark profiling method (ABI 310 Genetic Analyzer). The devices costed between USD 1–3 to fabricate and can be built within less than an hour.

C. Fully desktop-compatible fabrication of electrochemical microfluidic reactors

Charles Henry's group at Colorado State University developed a technique using a composite of dichloromethane-dissolved polycaprolactone (PCL) and graphite powder to embed electrodes within a microfluidic device[97] [Fig. 4(b)]. The PCL–carbon composites are shaped by pressing into laser-cut templates, and then the electrode layer is bonded to a laser-cut PMMA microfluidic part. The lower melting temperature of PCL relative to PMMA also enabled easy sealing strategy for the microfluidic device, as the parts are bonded through heat-pressing at 85 °C. Interestingly, instead of utilizing electrochemical microfluidics as a biosensor, this team demonstrated organic synthesis with said device. TEMPO-mediated oxidation of piperonyl alcohol into piperonal was performed through water-in-oil droplet microfluidic actuation and two-electrode electrolytic cells, achieving a conversion yield of 43%.

D. Fully desktop-compatible fabrication of electrochemical microfluidic biosensors

A group at Federal University of São Carlos, Brazil, have developed a 16-channel multiplexed electrochemical microfluidic biosensor, by using vinyl stencils and carbon/silver inks for the electrodes in a three electrode micro-cell, and paperfluidic circuits for sample metering and distribution.[77] All substrate material processing was performed on a Silhouette Cameo® 3 cutting plotter. The device takes in 60 μl of samples and distributes them into 16 volume metering pads of ~2 μl each. A subsequent work[184] demonstrated on-chip generation of quadruplicate measurements for glucose, creatinine, and uric acid, achieving limits of detection of 0.120, 0.084, and 0.012 mM respectively, with the fourth set of quadruplicate measurement reserved for controls.

Another work independent to Fava *et al.* also uses cutting plotter for electrochemical microfluidic biosensor fabrication. Jutiporn Yukird and colleagues at Chulalongkorn University, Thailand, and Sogang University, South Korea, developed a dual platform for detection of bisphenol A.[185] The biosensor device is fabricated by cutting continuous flow microchannels on pressure-sensitive adhesive (PSA), then sandwiched the PSA between a tape and a photopaper. The photopaper is pre-patterned using multi-walled carbon nanotube (MWCNT) ink for working and counter electrodes, and silver nanoparticle ink for the reference electrodes through direct ink writing (DIW) via the plotter and ballpoint pen. On the same platform, samples are split into an electrochemical sensor on the one side, and a zinc oxide-enhanced laser desorption ionization (LDI) target stage on the other side. The LDI stage is then inserted into an LDI-mass spectrometer instrument for analysis. Their platform exhibited detection capability for BPA at sample volume as low as 10 μl, with a detection limit of 0.35 μM for electrochemical detection and an ultralow detection limit of 0.01 pM for LDI-MS.

Wei Gao's group at Caltech applies a combination of laser-induced graphene electrodes on Kapton and laser-cut microfluidic channels on PET and medical tapes to fabricate a wearable sweat sensor patch capable of detecting uric acid and tyrosine levels, sweat rate estimation, temperature sensing, and pulse monitoring[131] [Fig. 4(c)]. The uric acid and tyrosine levels were measured through differential pulse voltammetry, the temperature sensing applies resistive thermal sensing, the pulse monitoring utilized piezoresistive strain measurements, and the sweat rate is estimated using optical analysis of sweat flow rate in microfluidics channels. The limits of detection for uric acid and tyrosine were 0.74 μM and 3.6 μM respectively, and the strain sensor remains stable after 10 000 bending cycles. A small pilot study on fitness monitoring and gout management were also performed, obtaining Pearson correlation coefficients of 0.963 and 0.864 against sweat and serum uric acid levels measured using high performance liquid chromatography (HPLC) as gold standard. Similar fabrication technique has been used by the same lab for development of sweat patch cortisol sensors[130] and rapid multiplexed antigen–antibody sensors for COVID-19 biomarkers.[186]

Figure 4 shows images of selected examples of microfluidic biosensors, including electrochemical and non-electrochemical ones, and prototyped through semi-cleanroom-dependent and fully desktop-compatible fabrication. Table III provides a summary of the relevant prior works.

VI. CONSIDERATIONS FOR SELECTING FRUGAL PROTOTYPING APPROACHES

There are several aspects to consider when deciding to invest in frugal microfabrication strategies, whether when starting out a laboratory or to transition away from conventional cleanroom-associated microfabrication techniques. A thorough assessment of these aspects should be performed prior to starting a project, weighing in the advantages and costs of investing in low-cost prototyping setups made available in-house vs pursuing subscription models for conventional fabrication facilities. An understanding of necessary specification of the microfabrication process helps to frame the project's suitability in favor of cleanrooms or non-cleanroom settings (e.g., makerspaces), and in the case of non-cleanroom settings, helps mitigate the deficiencies of the selected prototyping approach (relative to having cleanroom access).

A. Costs and accessibility of tools and facilities

Upfront costs, consumables and maintenance are among costs to consider when deciding a microfabrication approach. Desktop-compatible fabrication has the obvious advantage of low cost of

TABLE III. Summary of relevant prior works.

Prior work	Detection mode	Application	Fabrication technique employed	Outcomes
179	Electrochemical	Creatinine kinase-myocardial band (CK-MB) immunoassay	Metallization (Au–Au–Ag): sputtering through photoresist Microfluidics: laser-cut polyester film laminated with pressure-sensitive adhesive	• 4-step assay • Limit of detection: 0.25 ng ml^{-1}
174, 182	Electrochemical	Detection of serum miRNA-19b and miRNA-20a	Metallization (Pt–Pt–Ag): sputtering through shadow mask Microfluidics: laminated dry resist film	• Overall processing time of 4 h • Readout time of 9 min • LoD of 10 pM • Sample volume < 0.6 μl
122	Optical	Rubellavirus IgG immunoassay	Metallization (Ag): commercial inkjet printing Microfluidics: roll-to-roll coating of CEP dielectric and Fluoropel on electrode array	• 13-step assay • Cost: USD 0.63 per device • LoD: 0.02 IU ml^{-1}
183	Optical	HIV-1 RNA nucleic acid titer	Metallization (Ag): Dimatix inkjet printing on Kapton Microfluidics: nitrocellulose membranes in plastic, wax valves	• Cost: USD 2.23 per assay • Reusable components: USD 70 • LoD: 2.3×10^7 virus copies per ml
94, 95	Optical	DNA extraction, PCR amplification and electrophoretic separation for forensic DNA profiling	Metallization (Au): laser-cut gold leaf Microfluidics: laser-cut polyester film/PMMA/COC laminated using heat-sensitive adhesive	• Resolution: 2 base pairs • Separation distance: 40 mm • Cost: USD 1–3 • Fabrication time: < 1 h
97	Electrochemical	TEMPO-mediated oxidation of piperonyl alcohol into piperonal	Conductive element: polycaprolactone–carbon composite Microfluidics: laser-cut PMMA	• Bonding temperature: 85 °C • Conductivity: 200 S m^{-1} • Conversion yield: 43%
77, 184	Electrochemical	Glucose, creatinine and uric acid assay	Electrodes: DIW of carbon and Ag ink Microfluidics: filter paper in plastic enclosure	• 16-channel multiplexing

TABLE III. (*Continued.*)

Prior work	Detection mode	Application	Fabrication technique employed	Outcomes
• LoD: 0.120 mM (glucose), 0.084 mM (creatinine), 0.012 mM (uric acid)				
185	Electrochemical, mass spectrometric	Bisphenol A detection and LDI-MS sample preparation	Electrodes: DIW of carbon and Ag ink, ZnO surface modification Microfluidics: Laminated double-sided tape and photopaper	• Sample volume: 10 μl
• LoD (electrochemical): 0.35 μM • LoD (LDI-MS): 0.01 pM				
131	Electrochemical, piezoelectric, thermal, optical	Sweat uric acid and tyrosine level, body temperature, sweat rate analysis, pulse monitoring	Electrodes: laser-induced graphene Microfluidics: laser-cut, laminated PET and medical tape	• LoD: 0.74 μM (uric acid), 3.6 μM (tyrosine), 0.051 °C (temperature)
• Sensitivity: 3.5 μA mM^{-1} cm^{-2} (UA), 0.61 nA mM^{-1} cm^{-2} (Tyr), −0.06% °C^{-1} (temp.)				

facilities and equipment. Many of these techniques involve use of commercially available instrumentation such as 3D printers, laser cutter, office inkjet printers, laser-jet printers, cutting plotters, wax printers, and office laminators. Some of these equipment are relatively more expensive, such as material inkjet printers (e.g., Dimatix-2800 series), however it is still relatively cheaper than cleanroom equipment, such as photolithographic mask aligners, physical vapor deposition (PVD) chambers and plasma-enhanced chemical vapor deposition (PECVD) machines. Such equipments can also be operated in standard laboratory spaces, removing the need for a cleanroom facility, in which rental/subscription could cost few thousands annually, and building one such facility costs tens to hundreds of millions of dollars. Purchasing equipment to be used in-house also allow sustainable long-term use across multiple projects.

B. Processing time

In general, many frugal fabrication techniques have start-to-end processes that are faster or at par with a typical cleanroom fabrication. Frugal prototyping approaches in general has lesser procedural steps than cleanroom techniques, and faster iterative turnaround time between two iterations of a prototype. For example, a made-to-order custom silkscreen for screen-printing should takes around the same time to customize a chromium photomask for a cleanroom process, or faster thereof. Some techniques do have steps with long incubation time, for example, ESCARGOT's curing and mold dissolution time.[81]

C. Simplicity

Mastering cleanroom microfabrication processes can be a steep learning curve for personnel. On the other hand, desktop-compatible methods typically involve instrumentation that requires minimal training to setup and perform, and typically could be mastered with approximately 1–3 h of training. Some of these alternative techniques also use existing commonplace home/office equipment, as in the case of consumer-grade IJP platforms.[121] However, some of the methods still involve large learning curve, for example, the Dimatix IJP platforms, which require extensive pre-use optimization.[109] Additionally, some of these techniques, such as laminated microfluidic devices,[3] 3D-printed fluidics[2] and ESCARGOT[81] enable three-dimensional features and multilayered functionalities with lesser amount of steps as compared to using cleanroom techniques. Many of the low-cost equipment are also easy to repair and easily replaceable and has short downtimes (if any).

D. Mass manufacturing scalability and reproducibility

Non-automated cleanroom processes, which is common for cleanrooms outside mass-scale semiconductor fabrication plants, relies on manual intervention and human judgment at several processing steps, particularly, for photolithographic mask alignment and determining deposition exposure times. These interventions introduce human errors which may negatively affect repeatability and reproducibility. Microfabrication strategies with minimal human intervention during patterning steps will improve reproducibility, regardless of it being a cleanroom process or otherwise. Techniques such as screen-printing, inkjet printing and lamination are more easily parallelizable compared to cleanroom processes, and even converted into roll-to-roll printing,[187] which makes them suitable for upscaling to medium- and large-scale manufacturing of μTAS devices.

E. Resolution/dimensions of design features

The choice of device fabrication process is dependent on the design specifications. Cleanroom-associated processes enable fabrication of features at a higher resolution and/or aspect ratio.

Equipments such as electron-beam lithography enable features down to sub-10 nm resolutions,[188] which is crucial for nanofluidic, nano-mechanical sensors, and nanoelectronic applications. Most of the cleanroom-free techniques operate at the hundreds of micrometers in the scale, although some inkjet printing techniques can achieve sub-100 μm resolutions. When electing to fabricate devices using cleanroom-free approaches, it is advisable to have a general idea of the desired feature dimensions for the intended application.

F. Material versatility

Except for material inkjet printer platforms, cleanroom-free techniques typically have limited choice of materials compared to conventional cleanroom techniques, largely due to the techniques developed for non-generalizable sets of substrate and materials. A few examples include desktop printer methods limited to flexible substrates, screen-printing methods limited to available types of functional ink, and laminated sheets limited to specific thicknesses (which causes discrete channel heights). On the opposite, cleanroom-associated deposition technique works using high energy systems which enables deposition of metals and non-metals from a pure solid source, instead of aqueous colloids in the case of inkjet printing, or mixtures of conductive particles with binders and additives in the case of screen-printing, in which both require some optimization of formulation.[189–191] Sputtered materials typically form smoother and denser deposits compared to ink-based materials.[192,193] Cleanroom methods also enable very thin deposition of materials, down to sub-10 nm thicknesses that may result in superior electrical, thermal, and surface physicochemical properties.

G. Cleanliness

Among considerations required for microdevice fabrication is how much dust particles may affect the product. This effect becomes particularly significant at the sub-100 micronmeter scale. Outside a cleanroom, strategies such as laminar flow hoods may be employed to overcome dust issues. Access to surface cleaning instruments such as plasma cleaners or corona discharge guns, or lack thereof, may affect feasibility of microfabrication outside of a cleanroom. One study showed that protein immobilization efficiency is lower on polyester surface that has not been cleaned using plasma.[194] Additionally, usage of hazardous cleaning agents such as piranha solution for the preparation of substrates may be used, however, proper engineering controls and safe disposal protocols needs to be established—which in the case of most academic and commercial cleanrooms, are present by design, else, other safer substrate cleaning regimes (often more extensive) need to be considered.

VII. PERSPECTIVES AND OUTLOOK

The introduction of frugal science and innovation and its application in μTAS have provided an avenue for low-cost, accessible process for fabrication of electrochemical sensors among researchers in academia and industry, especially, in low- and medium-income countries (LMICs). The approach of frugal science, or "constraint-based science", often starts by asking questions about costs, accessibility, and inclusivity and leads to an innovator's ability to reframe problems and solutions.[195,196] Some of the prominent frugal innovations in science tools have revolutionized how we perceive microscopes,[197,198] centrifuges,[199] and electroporators[135] could be used in real world applications. Within the field of microdevices and biosensors, a common approach is to develop "tools to create tools," usually kits containing modular parts for non-specialists to build custom microfluidic circuits and diagnostic kits. A few well-known examples of this is Ampli, which is based on laser-cut lateral flow assay modules[200] and micromachined Lego bricks.[201] For microfabrication, in general, several "cleanroom-to-makerspaces" approaches have been introduced, as reviewed by Walsh *et al.*[1]

As the barriers to cost and accessibility to sensor and microdevices prototyping are lowered, more exploratory and educational work on chemical and biological sensing may take place. Among the benefactors of the approaches mentioned in this review are researchers from non-microfluidic background that intends to explore microfluidics in their applications in a low-cost and low-risk approach, as well as early career researchers and educators with financial constraints. The approaches for low-cost prototyping of microdevices already found its applications in education. Rackus, Riedel-Kruse, and Pamme recently wrote a review on the use of microfluidics in public education and formal classroom settings, classifying easily scalable microfluidic prototypes appropriate to science festivals, workshop sessions, or undergraduate teaching labs.[202] Chatmontree and colleagues demonstrated use of paper microfluidic battery as means to teach electrochemistry at the middle school level.[203]

The utility of low-cost prototyping is not limited only to educational purposes. Low-cost prototyping techniques have been used in basic biology research, such as fruit fly embryo culture in laminated foil bioreactors for developmental biology study[204] and paperfluidic devices for nematode drug studies.[205] Additionally, proofs of concept for diagnostic devices made using the techniques mentioned in this review have been demonstrated and validated using clinical samples.[206–208] Early prototyping using desktop-compatible prototyping techniques[122,209] have also led to pilot studies that has been deployed into field settings.[13,210,211]

Low-cost microfabrication allows rapid response to emerging global challenges whenever necessary. The recent COVID-19 pandemic led to emergence of multiple independent solutions to mass testing, in order to overcome the bottleneck of RT-PCR testing capacity in central laboratories.[212,213] Many of such innovations, especially, in the context of those stemming from academic research groups, utilized low-cost prototyping methods to validate novel test kits in pilot studies.[186,214] These studies are often expedited and executed at low- to medium-scale using real patient samples and play significant role in derisking the technology to expand in the scale.

For researchers in under-resourced institutions, especially, in LMICs, project costs are non-negligible. Cleanroom-associated instruments such as UV photolithography mask aligners and sputtering chambers may cost anywhere from USD 10 000 to several millions of dollars, while membership access to the few available cleanroom facilities may cost several thousands of dollars per annum, non-inclusive of consumables. Biorecognition molecules are often functionalized onto the device or sensors using microarray spotter, a costly robotic instrumentation meant for customizing

nucleic acid microarrays,[215] which led to the development of a lower cost spotting device.[144,216] Even medium-cost instruments such as the Dimatix multimaterial inkjet printers involve a significant starting investment, as compared to commercial hobbyist equipments such as 3D printers, laser engravers, and cutting plotters. While many of higher end innovation and commercialization in the μTAS subfield has been concentrated primarily in high income countries, it is not surprising that the development at the extreme low cost of microfabrication has been spearheaded by researchers in LMIC countries such as India, Vietnam, and Thailand.[71,79,144,185] Within a restricted scope of design specification, low-cost methods are able emulate cleanroom-based microfabrication of biosensors at the benchtop/desktop, with a low upfront and consumable cost and easy-to-access materials and tools.

An important aspect to note is that many of these sensors rely on instruments that could decipher the transduced signals from the sensors, such as potentiostats (for electrochemical sensors), spectrometers (optical sensors), and impedance meters (piezoresistive sensors). Fortunately, just as low-cost prototyping of sensors is increasingly maturing as a subfield, so does low-cost, open-source instrumentation. Some of the examples of recent developments are the DStat[217] and KickStat[218] potentiostats, the openQCM[53] piezoelectric frequency monitor, as well as CMOS optical sensors sourced from commercial webcams[219] and Raspberry Pi camera modules.[197] These new instruments, as well as their commercial counterparts, have been validated to perform, and their integration with low-cost microfabrication approaches present an affordable option to under-resourced researchers to pursue miniaturized biological and chemical sensor research and development.

As the adoption of low-cost, cleanroom-free microfabrication techniques increases across the globe, we envision that the research and development of biological and chemical sensors will proliferate, finding end consumer applications in fields such as biomedicine, food technology, environmental monitoring, and industrial manufacturing.

ACKNOWLEDGMENTS

This work is financially supported by the Asian Office of Aerospace Research and Development (AOARD, Grant No. 16IOA040), Tokyo, Japan.

AUTHOR DECLARATIONS

Conflict of Interest

The authors have no conflicts of interest to disclose.

DATA AVAILABILITY

Data sharing is not applicable to this article as no new data were created or analyzed in this study.

REFERENCES

[1]D. I. Walsh, D. S. Kong, S. K. Murthy, and P. A. Carr, Trends Biotechnol. **35**, 383 (2017).
[2]N. Bhattacharjee, A. Urrios, S. Kang, and A. Folch, Lab Chip **16**, 1720 (2016).
[3]M. Focke, D. Kosse, C. Müller, H. Reinecke, R. Zengerle, and F. von Stetten, Lab Chip **10**, 1365 (2010).
[4]N. Bhalla, P. Jolly, N. Formisano, and P. Estrela, Essays Biochem. **60**, 1 (2016).
[5]A. P. F. Turner, Chem. Soc. Rev. **42**, 3184 (2013).
[6]R. Franco-Duarte, L. Černáková, S. Kadam, K. S. Kaushik, B. Salehi, A. Bevilacqua, M. R. Corbo, H. Antolak, K. Dybka-Stępień, M. Leszczewicz, S. Relison Tintino, V. C. Alexandrino de Souza, J. Sharifi-Rad, H. D. Melo Coutinho, N. Martins, and C. F. Rodrigues, Microorganisms **7**, 130 (2019).
[7]N. Singhal, M. Kumar, P. K. Kanaujia, and J. S. Virdi, Front. Microbiol. **6**, 791 (2015).
[8]Y. V. Medvedev, G. V. Ramenskaya, I. E. Shokhin, and T. A. Yarushok, Pharm. Chem. J. **47**, 225 (2013).
[9]J. R. Priest, Curr. Opin. Pediatr. **29**, 513 (2017).
[10]S. Chen and M. H. Shamsi, J. Micromech. Microeng. **27**, 083001 (2017).
[11]N. A. Bhuiyan, F. Qadri, A. S. G. Faruque, M. A. Malek, M. A. Salam, F. Nato, J. M. Fournier, S. Chanteau, D. A. Sack, and G. Balakrish Nair, J. Clin. Microbiol. **41**, 3939 (2003).
[12]M. H. Mat Zaid, J. Abdullah, N. A. Yusof, Y. Sulaiman, H. Wasoh, M. F. Md Noh, and R. Issa, Sens. Actuators, B **241**, 1024 (2017).
[13]A. H. C. Ng, R. Fobel, C. Fobel, J. Lamanna, D. G. Rackus, A. Summers, C. Dixon, M. D. M. Dryden, C. Lam, M. Ho, N. S. Mufti, V. Lee, M. A. M. Asri, E. A. Sykes, M. D. Chamberlain, R. Joseph, M. Ope, H. M. Scobie, A. Knipes, P. A. Rota, N. Marano, P. M. Chege, M. Njuguna, R. Nzunza, N. Kisangau, J. Kiogora, M. Karuingi, J. W. Burton, P. Borus, E. Lam, and A. R. Wheeler, Sci. Transl. Med. **10**, eaar6076 (2018).
[14]N. T. Q. Nhu, D. Heemskerk, D. D. A. Thu, T. T. H. Chau, N. T. H. Mai, H. D. T. Nghia, P. P. Loc, D. T. M. Ha, L. Merson, T. T. V. Thinh, J. Day, N. v. V. Chau, M. Wolbers, J. Farrar, and M. Caws, J. Clin. Microbiol. **52**, 226 (2014).
[15]S. W. Dutse, N. A. Yusof, H. Ahmad, M. Z. Hussein, Z. Zainal, R. Hushiarian, and R. Hajian, Anal. Lett. **47**, 819 (2014).
[16]Y. Kawahara, H. Lee, and M. M. Tentzeris, in *UbiComp'12—Proceedings of the 2012 ACM Conference on Ubiquitous Computing* (ACM, 2012), p. 545.
[17]J. Lin, M. Wang, M. Zhang, Y. Zhang, and L. Chen, in *Computer and Computing Technologies in Agriculture, Volume II*, edited by D. Li (Springer US, Boston, MA, 2008), pp. 1349–1353.
[18]B. M. Paddle, Biosens. Bioelectron. **11**, 1079 (1996).
[19]A. Avramescu, S. Andreescu, T. Noguer, C. Bala, D. Andreescu, and J.-L. Marty, Anal. Bioanal. Chem. **374**, 25 (2002).
[20]V. Venugopal, Biosens. Bioelectron. **17**, 147 (2002).
[21]E. d. S. Gil and G. R. d. Melo, Braz. J. Pharm. Sci. **46**, 375 (2010).
[22]D. Yu, B. Blankert, J. Viré, and J. Kauffmann, Anal. Lett. **38**, 1687 (2005).
[23]Y. Liu, Y. Zhuang, D. Ding, Y. Xu, J. Sun, and D. Zhang, ACS Synth. Biol. **6**, 837 (2017).
[24]J. W. Rutter, T. Ozdemir, L. M. Quintaneiro, G. Thomas, F. Cabreiro, and C. P. Barnes, *Detecting Changes in the Caenorhabditis Elegans Intestinal Environment Using an Engineered Bacterial Biosensor* (Synthetic Biology, 2019).
[25]M. A. Morales and J. M. Halpern, Bioconjugate Chem. **29**, 3231 (2018).
[26]D. G. Rackus, M. H. Shamsi, and A. R. Wheeler, Chem. Soc. Rev. **44**, 5320 (2015).
[27]S. Daniele and C. Bragato, in *Environmental Analysis by Electrochemical Sensors and Biosensors*, edited by L. M. Moretto and K. Kalcher (Springer, New York, NY, 2014), pp. 373–401.
[28]C.-C. Chang and R.-J. Yang, Microfluid Nanofluid **3**, 501 (2007).
[29]K. Hiramoto, K. Ino, Y. Nashimoto, K. Ito, and H. Shiku, Front. Chem. **7**, 396 (2019).
[30]N. J. Ronkainen, H. B. Halsall, and W. R. Heineman, Chem. Soc. Rev. **39**, 1747 (2010).
[31]U. Mohd Azmi, N. Yusof, N. Kusnin, J. Abdullah, S. Suraiya, P. Ong, N. Ahmad Raston, S. Abd Rahman, and M. Mohamad Fathil, Sensors **18**, 3926 (2018).
[32]M. H. Shamsi, K. Choi, A. H. C. Ng, and A. R. Wheeler, Lab Chip **14**, 547 (2014).
[33]G. Li and P. Miao, *Theoretical Background of Electrochemical Analysis* (Springer, 2013), pp. 5–18; avaialable at http://link.springer.com/10.1007/978-3-642-34252-3_2.

[34]N. Elgrishi, K. J. Rountree, B. D. McCarthy, E. S. Rountree, T. T. Eisenhart, and J. L. Dempsey, J. Chem. Educ. **95**, 197 (2018).
[35]L. Manjakkal, D. Shakthivel, and R. Dahiya, Adv. Mater. Technol. **3**, 1800252 (2018).
[36]S. Sarkar, S. Lai, and S. Lemay, Micromachines **7**, 81 (2016).
[37]A. Fernández-la-Villa, D. F. Pozo-Ayuso, and M. Castaño-Álvarez, Curr. Opin. Electrochem. **15**, 175 (2019).
[38]S. Khan, L. Lorenzelli, and R. S. Dahiya, IEEE Sens. J. **15**, 3164 (2015).
[39]Q. Li, J. Zhang, Q. Li, G. Li, X. Tian, Z. Luo, F. Qiao, X. Wu, and J. Zhang, Front. Mater. **5**, 77 (2019).
[40]K. Yamanaka, M. Vestergaard, and E. Tamiya, Sensors **16**, 1761 (2016).
[41]F. Arduini, L. Micheli, D. Moscone, G. Palleschi, S. Piermarini, F. Ricci, and G. Volpe, Trends Anal. Chem. **79**, 114 (2016).
[42]A. F. M. Mansor, I. Ibrahim, A. A. Zainuddin, I. Voiculescu, and A. N. Nordin, Med. Biol. Eng. Comput. **56**, 173 (2018).
[43]A. Tretjakov, V. Syritski, J. Reut, R. Boroznjak, and A. Öpik, Anal. Chim. Acta **902**, 182 (2016).
[44]S. M. Restaino and I. M. White, Anal. Chim. Acta **1060**, 17 (2019).
[45]J. F. C. Loo, A. H. P. Ho, A. P. F. Turner, and W. C. Mak, Trends Biotechnol. **37**, 1104 (2019).
[46]R. W. Peeling, K. K. Holmes, D. Mabey, and A. Ronald, Sex. Transm. Infect. **82**, v1 (2006).
[47]G. J. Sommer, D. S. Chang, A. Jain, S. M. Langelier, J. Park, M. Rhee, F. Wang, R. I. Zeitoun, and M. A. Burns, *Microfluidics for Biological Applications* (Springer US, Boston, MA, 2009), pp. 1–34.
[48]S. Yasotharan, S. Pinto, J. G. Sled, S.-S. Bolz, and A. Günther, Lab Chip **15**, 2660 (2015).
[49]J. L. Osborn, B. Lutz, E. Fu, P. Kauffman, D. Y. Stevens, and P. Yager, Lab Chip **10**, 2659 (2010).
[50]Z. Li, J. Huang, B. Yang, Q. You, S. Sekine, D. Zhang, and Y. Yamaguchi, Sens. Actuators, B **254**, 153 (2018).
[51]A. J. Hughes and A. E. Herr, Proc. Natl. Acad. Sci. U.S.A. **109**, 21450 (2012).
[52]J. S. Farrar and C. T. Wittwer, Clin. Chem. **61**, 145 (2015).
[53]A. Anwar Zainuddin, A. N. Nordin, R. A. Rahim, A. A. M. Ralib, S. Khan, C. Guines, M. Chatras, and A. Pothier, Indones. J. Electr. Eng. Comput. Sci. **10**, 84 (2018).
[54]K. Krorakai, S. Klangphukhiew, S. Kulchat, and R. Patramanon, Appl. Sci. **11**, 392 (2021).
[55]T. Laksanasopin, T. W. Guo, S. Nayak, A. A. Sridhara, S. Xie, O. O. Olowookere, P. Cadinu, F. Meng, N. H. Chee, J. Kim, C. D. Chin, E. Munyazesa, P. Mugwaneza, A. J. Rai, V. Mugisha, A. R. Castro, D. Steinmiller, V. Linder, J. E. Justman, S. Nsanzimana, and S. K. Sia, Sci. Transl. Med. **7**, 273re1 (2015).
[56]D. R. Reyes, D. Iossifidis, P. A. Auroux, and A. Manz, Anal. Chem. **74**, 2623 (2002).
[57]A. Noori, S. Upadhyaya, and P. R. Selvanganapathy, *Microfluidics for Biological Applications* (Springer US, Boston, MA, 2009), pp. 35–92.
[58]Y. Xia and G. M. Whitesides, Angew. Chem., Int. Ed. **37**, 550 (1998).
[59]H. N. Chan, Y. Chen, Y. Shu, Y. Chen, Q. Tian, and H. Wu, Microfluidics Nanofluidics **19**, 9 (2015).
[60]P. G. Shankles, L. J. Millet, J. A. Aufrecht, and S. T. Retterer, PLoS One **13**, e0192752 (2018).
[61]M. E. Wilson, N. Kota, Y. Kim, Y. Wang, D. B. Stolz, P. R. LeDuc, and O. B. Ozdoganlar, Lab Chip **11**, 1550 (2011).
[62]K. Stephan, P. Pittet, L. Renaud, P. Kleimann, P. Morin, N. Ouaini, and R. Ferrigno, J. Micromech. Microeng. **17**, N69 (2007).
[63]S. K. Sia and G. M. Whitesides, Electrophoresis **24**, 3563 (2003).
[64]U. M. Attia, S. Marson, and J. R. Alcock, Microfluid Nanofluid **7**, 1 (2009).
[65]S. Yang and D. L. DeVoe, in *Microfluidic Diagnostics*, edited by G. Jenkins and C. D. Mansfield (Humana Press, Totowa, NJ, 2013), pp. 115–123.
[66]F. Yu and D. Choudhury, Drug Discov. Today **24**, 1248 (2019).
[67]T. Pan and W. Wang, Ann. Biomed. Eng. **39**, 600 (2011).
[68]A. W. Martinez, S. T. Phillips, M. J. Butte, and G. M. Whitesides, Angew. Chem., Int. Ed. Engl. **46**, 1318 (2007).
[69]X. Li, D. R. Ballerini, and W. Shen, Biomicrofluidics **6**, 011301 (2012).
[70]J. Potter, P. Brisk, and W. H. Grover, Lab Chip **19**, 2000 (2019).
[71]N. K. Mani, A. Prabhu, S. K. Biswas, and S. Chakraborty, Sci. Rep. **9**, 1752 (2019).
[72]N. R. Pollock, J. P. Rolland, S. Kumar, P. D. Beattie, S. Jain, F. Noubary, V. L. Wong, R. A. Pohlmann, U. S. Ryan, and G. M. Whitesides, Sci. Transl. Med. **4**, 152ra129 (2012).
[73]B. R. Lutz, P. Trinh, C. Ball, E. Fu, and P. Yager, Lab Chip **11**, 4274 (2011).
[74]E. Fu, T. Liang, P. Spicar-Mihalic, J. Houghtaling, S. Ramachandran, and P. Yager, Anal. Chem. **84**, 4574 (2012).
[75]V. N. Ataide, L. F. Mendes, L. I. L. M. Gama, W. R. de Araujo, and T. R. L. C. Paixão, Anal. Methods **12**(8), 1030 (2020).
[76]C.-C. Wang, J. W. Hennek, A. Ainla, A. A. Kumar, W.-J. Lan, J. Im, B. S. Smith, M. Zhao, and G. M. Whitesides, Anal. Chem. **88**, 6326 (2016).
[77]E. L. Fava, T. A. Silva, T. M. D. Prado, F. C. de Moraes, R. C. Faria, and O. Fatibello-Filho, Talanta **203**, 280 (2019).
[78]H.-T. Nguyen, H. Thach, E. Roy, K. Huynh, and C. Perrault, Micromachines **9**, 461 (2018).
[79]H. Thach, H.-T. Nguyen, U. Tong, T. Hoang, T.-A. Vuong, C. M. Perrault, and K. Huynh, "Comparison of nail Polish meth(acrylates) (MA) gel photoresist and vinyl adhesive paper for low-cost microfluidics fabrication," in *7th International Conference on the Development of Biomedical Engineering in Vietnam (BME7)* (Springer, 2020).
[80]P. Mukherjee, F. Nebuloni, H. Gao, J. Zhou, and I. Papautsky, Micromachines **10**, 192 (2019).
[81]V. Saggiomo and A. H. Velders, Adv. Sci. **2**, 1500125 (2015).
[82]M. Rafeie, M. Welleweerd, A. Hassanzadeh-Barforoushi, M. Asadnia, W. Olthuis, and M. Ebrahimi Warkiani, Biomicrofluidics **11**, 014108 (2017).
[83]K. Kang, S. Oh, H. Yi, S. Han, and Y. Hwang, Biomicrofluidics **12**, 014105 (2018).
[84]L. K. Fiddes, H. K. C. Chan, B. Lau, E. Kumacheva, and A. R. Wheeler, Biomaterials **31**, 315 (2010).
[85]A. Grimes, D. N. Breslauer, M. Long, J. Pegan, L. P. Lee, and M. Khine, Lab Chip **8**, 170 (2008).
[86]C.-S. Chen, D. N. Breslauer, J. I. Luna, A. Grimes, W. Chin, L. P. Lee, and M. Khine, Lab Chip **8**, 622 (2008).
[87]A. Chen, D. K. Lieu, L. Freschauf, V. Lew, H. Sharma, J. Wang, D. Nguyen, I. Karakikes, R. J. Hajjar, A. Gopinathan, E. Botvinick, C. C. Fowlkes, R. A. Li, and M. Khine, Adv. Mater. **23**, 5785 (2011).
[88]T. Wang, T. U. Luu, A. Chen, M. Khine, and W. F. Liu, Biomater. Sci. **4**, 948 (2016).
[89]D. A. Bartholomeusz, R. W. Boutté, and J. D. Andrade, J. Microelectromech. Syst. **14**, 1364 (2005).
[90]A. W. Taylor and D. M. Harris, Rev. Sci. Instrum. **90**, 116102 (2019).
[91]P. K. Yuen and V. N. Goral, Lab Chip **10**, 384 (2010).
[92]B. L. Thompson, Y. Ouyang, G. R. M. Duarte, E. Carrilho, S. T. Krauss, and J. P. Landers, Nat. Protoc. **10**, 875 (2015).
[93]Y. Ouyang, J. Li, C. Phaneuf, P. S. Riehl, C. Forest, M. Begley, D. M. Haverstick, and J. P. Landers, Lab Chip **16**, 377 (2016).
[94]B. L. Thompson, C. Birch, D. A. Nelson, J. Li, J. A. DuVall, D. Le Roux, A.-C. Tsuei, D. L. Mills, B. E. Root, and J. P. Landers, Lab Chip **16**, 4569 (2016).
[95]C. Birch, J. A. DuVall, D. Le Roux, B. L. Thompson, A. C. Tsuei, J. Li, D. A. Nelson, D. L. Mills, J. P. Landers, and B. E. Root, Micromachines **8**, 17 (2017).
[96]B. L. Thompson, C. Birch, J. Li, J. A. DuVall, D. Le Roux, D. A. Nelson, A.-C. Tsuei, D. L. Mills, S. T. Krauss, B. E. Root, and J. P. Landers, Analyst **141**, 4667 (2016).
[97]K. J. Klunder, K. M. Clark, C. McCord, K. E. Berg, S. D. Minteer, and C. S. Henry, Lab Chip **19**, 2589 (2019).
[98]A. Lashkaripour, R. Silva, and D. Densmore, Microfluid. Nanofluid. **22**, 31 (2018).

[99]X. Liu, Z. Dong, Q. Zhao, and G. Li, Microfluid. Nanofluid. **24**, 11 (2020).
[100]X. Ku, Z. Zhang, X. Liu, L. Chen, and G. Li, Microfluid. Nanofluid. **22**, 82 (2018).
[101]P. K. Yuen and V. N. Goral, J. Chem. Educ. **89**, 1288 (2012).
[102]S. Franssila, *Introduction to Microfabrication: Franssila/Introduction to Microfabrication* (John Wiley & Sons, Ltd, Chichester, UK, 2010).
[103]J. Shao, X. Chen, X. Li, H. Tian, C. Wang, and B. Lu, Sci. China Technol. Sci. **62**, 175 (2019).
[104]K. Petherbridge, P. Evans, and D. Harrison, Circuit World **31**, 41 (2005).
[105]S. J. Williams, N. Romero, L. Parkes, D. J. Jackson, and J. F. Naber, J. Electrostat. **75**, 49 (2015).
[106]W. K. Tomazelli Coltro, J. A. Fracassi da Silva, and E. Carrilho, Anal. Methods **3**, 168 (2011).
[107]M. Abdelgawad and A. R. Wheeler, Microfluid Nanofluid **4**, 349 (2008).
[108]G. Dutta, A. A. Jallow, D. Paul, and D. Moschou, Micromachines **10**, 575 (2019).
[109]A. A. Zainuddin, A. F. M. Mansor, R. A. Rahim, and A. N. Nordin, AIP Conf. Proc. **1808**, 020066 (2017).
[110]S. Siddiquee, K. Rovina, N. A. Yusof, K. F. Rodrigues, and S. Suryani, Sens. Bio-Sens. Res. **2**, 16 (2014).
[111]P. D. Sinawang, L. Fajs, K. Elouarzaki, J. Nugraha, and R. S. Marks, Sens. Actuators, B **259**, 354 (2018).
[112]X. Fan, W. Nie, H. Tsai, N. Wang, H. Huang, Y. Cheng, R. Wen, L. Ma, F. Yan, and Y. Xia, Adv. Sci. **6**, 1900813 (2019).
[113]H. Wang, J. Lin, and Z. X. Shen, J. Sci.: Adv. Mater. Dev. **1**, 225 (2016).
[114]Z. Taleat, A. Khoshroo, and M. Mazloum-Ardakani, Microchim. Acta **181**, 865 (2014).
[115]L. Monkkonen, J. S. Edgar, D. Winters, S. R. Heron, C. L. Mackay, C. D. Masselon, A. A. Stokes, P. R. R. Langridge-Smith, and D. R. Goodlett, J. Chromatogr., A **1439**, 161 (2016).
[116]A. N. Nordin, A. A. Zainuddin, R. A. Rahim, I. Voiculescu, and W. C. Mak, Proc. Technol. **27**, 100 (2017).
[117]J. Li, F. Rossignol, and J. Macdonald, Lab Chip **15**, 2538 (2015).
[118]P. M. Grubb, H. Subbaraman, S. Park, D. Akinwande, and R. T. Chen, Sci. Rep. **7**, 1202 (2017).
[119]J. Sumerel, J. Lewis, A. Doraiswamy, L. F. Deravi, S. L. Sewell, A. E. Gerdon, D. W. Wright, and R. J. Narayan, Biotechnol. J. **1**, 976 (2006).
[120]W. Su, B. S. Cook, Y. Fang, and M. M. Tentzeris, Sci. Rep. **6**, 35111 (2016).
[121]Y. Kawahara, S. Hodges, N.-W. Gong, S. Olberding, and J. Steimle, IEEE Pervasive Comput. **13**, 30 (2014).
[122]C. Dixon, A. H. C. Ng, R. Fobel, M. B. Miltenburg, and A. R. Wheeler, Lab Chip **16**, 4560 (2016).
[123]B. Andò, S. Baglio, A. R. Bulsara, T. Emery, V. Marletta, and A. Pistorio, Sensors (Basel, Switzerland) **17**, 748 (2017).
[124]S. T. Krauss, T. P. Remcho, E. Monazami, B. L. Thompson, P. Reinke, M. R. Begley, and J. P. Landers, Anal. Methods **8**, 7061 (2016).
[125]V. Soum, H. Cheong, K. Kim, Y. Kim, M. Chuong, S. R. Ryu, P. K. Yuen, O.-S. Kwon, and K. Shin, ACS Omega **3**, 16866 (2018).
[126]K.-H. Choi, H.-W. Kim, S.-S. Lee, J. Yoo, D.-G. Lee, and S.-Y. Lee, Adv. Sustainable Syst. **2**, 1700132 (2018).
[127]J. Lin, Z. Peng, Y. Liu, F. Ruiz-Zepeda, R. Ye, E. L. G. Samuel, M. J. Yacaman, B. I. Yakobson, and J. M. Tour, Nat. Commun. **5**, 5714 (2014).
[128]L. Huang, J. Su, Y. Song, and R. Ye, Nano-Micro Lett. **12**, 157 (2020).
[129]N. Kurra, Q. Jiang, P. Nayak, and H. N. Alshareef, Nano Today **24**, 81 (2019).
[130]R. M. Torrente-Rodríguez, J. Tu, Y. Yang, J. Min, M. Wang, Y. Song, Y. Yu, C. Xu, C. Ye, W. W. IsHak, and W. Gao, Matter **2**, 921 (2020).
[131]Y. Yang, Y. Song, X. Bo, J. Min, O. S. Pak, L. Zhu, M. Wang, J. Tu, A. Kogan, H. Zhang, T. K. Hsiai, Z. Li, and W. Gao, Nat. Biotechnol. **38**, 217 (2020).
[132]H.-L. (Cindy) Kao, C. Holz, A. Roseway, A. Calvo, and C. Schmandt, in *Proceedings of the 2016 ACM International Symposium on Wearable Computers—ISWC '16* (ACM, 2016), p. 16.
[133]M. S. F. Santos, W. A. Ameku, I. G. R. Gutz, and T. R. L. C. Paixão, Talanta **179**, 507 (2018).
[134]Y. Wang, Z. Pei, M. Zhu, Z. Liu, Y. Huang, Z. Ruan, Y. Huang, Y. Zhao, S. Du, and C. Zhi, ACS Appl. Mater. Interfaces **10**, 21297 (2018).
[135]G. Byagathvalli, S. Sinha, Y. Zhang, M. P. Styczynski, J. Standeven, and M. S. Bhamla, PLoS Biol. **18**, e3000589 (2020).
[136]M. Lambrichts, J. M. Tijerina, T. De Weyer, and R. Ramakers, in *Proceedings of the Fourteenth International Conference on Tangible, Embedded, and Embodied Interaction* (ACM, Sydney, 2020), pp. 565–571.
[137]V. Perumal and D. Wigdor, in *Proceedings of the 28th Annual ACM Symposium on User Interface Software & Technology—UIST '15* (ACM Press, Daegu, 2015), pp. 243–251.
[138]A. Mohammadzadeh, A. E. Fox Robichaud, and P. R. Selvaganapathy, J. Microelectromech. Syst. **28**, 597 (2019).
[139]L. Song, M. Connolly, M. L. Fernández-Cruz, M. G. Vijver, M. Fernández, E. Conde, G. R. de Snoo, W. J. G. M. Peijnenburg, and J. M. Navas, Nanotoxicology **8**, 383 (2014).
[140]S. Nagels, R. Ramakers, K. Luyten, and W. Deferme, in *Proceedings of the 2018 CHI Conference on Human Factors in Computing Systems—CHI '18* (ACM Press, Montreal QC, 2018), pp. 1–13.
[141]D. McIntyre, A. Lashkaripour, and D. Densmore, Lab Chip **20**, 3690 (2020).
[142]J. Kudr, O. Zitka, M. Klimanek, R. Vrba, and V. Adam, Sens. Actuators, B **246**, 578 (2017).
[143]H.-L. (Cindy) Kao and MIT Media Lab, DuoSkin—Cindy Hsin-Liu Kao (n.d.). Accessed 2 Dec. 2020.
[144]N. Nuchtavorn and M. Macka, Anal. Chim. Acta **919**, 70 (2016).
[145]D. Kim and A. E. Herr, Biomicrofluidics **7**, 041501 (2013).
[146]D. Jung, S. Yeo, J. Kim, B. Kim, B. Jin, and D.-Y. Ryu, Surf. Coat. Technol. **200**, 2886 (2006).
[147]Y. H. Youn, S. J. Lee, G. R. Choi, H. R. Lee, D. Lee, D. N. Heo, B.-S. Kim, J. B. Bang, Y.-S. Hwang, V. M. Correlo, R. L. Reis, S. G. Im, and I. K. Kwon, Mater. Sci. Eng., C **100**, 949 (2019).
[148]W. Norde, Adv. Colloid Interface Sci. **25**, 267 (1986).
[149]S. A. Bhakta, E. Evans, T. E. Benavidez, and C. D. Garcia, Anal. Chim. Acta **872**, 7 (2015).
[150]F. Wieland, R. Bruch, M. Bergmann, S. Partel, G. A. Urban, and C. Dincer, Polymers **12**, 104 (2020).
[151]M. J. Fischer, *Methods in Molecular Biology* (Springer, Clifton, NJ, 2010), Vol. 627, p. 55.
[152]C. Wang, Q. Yan, H.-B. Liu, X.-H. Zhou, and S.-J. Xiao, Langmuir **27**, 12058 (2011).
[153]J. Cecchetto, F. C. Carvalho, A. Santos, F. C. B. Fernandes, and P. R. Bueno, Sens. Actuators, B **213**, 150 (2015).
[154]B. Feyssa, C. Liedert, L. Kivimaki, L.-S. Johansson, H. Jantunen, and L. Hakalahti, PLoS One **8**, e68918 (2013).
[155]I. Migneault, C. Dartiguenave, M. J. Bertrand, and K. C. Waldron, BioTechniques **37**, 790 (2004).
[156]K. Kim, S. W. Park, and S. S. Yang, BioChip J. **4**, 148 (2010).
[157]L. Tang and N. Y. Lee, Lab Chip **10**, 1274 (2010).
[158]J. M. Taylor, K. Perez-Toralla, R. Aispuro, and S. A. Morin, Adv. Mater. **30**, 1705333 (2018).
[159]J. C. Love, L. A. Estroff, J. K. Kriebel, R. G. Nuzzo, and G. M. Whitesides, Chem. Rev. **105**, 1103 (2005).
[160]Y. H. Tan, J. R. Schallom, N. V. Ganesh, K. Fujikawa, A. V. Demchenko, and K. J. Stine, Nanoscale **3**, 3395 (2011).
[161]D. K. Aswal, S. Lenfant, D. Guerin, J. V. Yakhmi, and D. Vuillaume, Anal. Chim. Acta **568**, 84 (2006).
[162]L. D. Burke and P. F. Nugent, Gold Bull. **30**, 43 (1997).
[163]L. D. Burke and P. F. Nugent, Gold Bull. **31**, 39 (1998).
[164]H. Häkkinen, Nat. Chem. **4**, 443 (2012).
[165]J. Stettner and A. Winkler, Langmuir **26**, 9659 (2010).
[166]A. T. Sage, J. D. Besant, B. Lam, E. H. Sargent, and S. O. Kelley, Acc. Chem. Res. **47**, 2417 (2014).

[167]S. Asiaei, P. Nieva, and M. M. Vijayan, J. Phys. Chem. B **118**, 13697 (2014).
[168]J. Suthar, E. S. Parsons, B. W. Hoogenboom, G. R. Williams, and S. Guldin, Anal. Chem. **92**, 4082 (2020).
[169]T. Sano, S. Vajda, and C. R. Cantor, J. Chromatogr. B: Biomed. Sci. Appl. **715**, 85 (1998).
[170]P. S. Stayton, S. Freitag, L. A. Klumb, A. Chilkoti, V. Chu, J. E. Penzotti, R. To, D. Hyre, I. Le Trong, T. P. Lybrand, and R. E. Stenkamp, Biomol. Eng. **16**, 39 (1999).
[171]J. A. Bornhorst and J. J. Falke, *Methods in Enzymology* (Elsevier, 2000), pp. 245–254.
[172]R. Ahmad, O. S. Wolfbeis, Y.-B. Hahn, H. N. Alshareef, L. Torsi, and K. N. Salama, Mater. Today Commun. **17**, 289 (2018).
[173]G. Zhu, H. Wang, and L. Zhang, Chem. Phys. Lett. **649**, 15 (2016).
[174]R. Bruch, A. Kling, G. A. Urban, and C. Dincer, J. Vis. Exp. **127**, e56105 (2017).
[175]J. Hui, J. Cui, G. Xu, S. B. Adeloju, and Y. Wu, Mater. Lett. **108**, 88 (2013).
[176]Y. Peng, C.-W. Wei, Y.-N. Liu, and J. Li, Analyst **136**, 4003 (2011).
[177]A. J. Bandodkar, P. Gutruf, J. Choi, K. Lee, Y. Sekine, J. T. Reeder, W. J. Jeang, A. J. Aranyosi, S. P. Lee, J. B. Model, R. Ghaffari, C.-J. Su, J. P. Leshock, T. Ray, A. Verrillo, K. Thomas, V. Krishnamurthi, S. Han, J. Kim, S. Krishnan, T. Hang, and J. A. Rogers, Sci. Adv. **5**, eaav3294 (2019).
[178]E. L. I. Santos, M. Rostro-Alanís, R. Parra-Saldívar, and A. J. Alvarez, Bioresour. Technol. **247**, 165 (2018).
[179]J. Kim, Y. Shin, S. Song, J. Lee, and J. Kim, Sens. Actuators, B **202**, 60 (2014).
[180]A. Fragoso, D. Latta, N. Laboria, F. von Germar, T. E. Hansen-Hagge, W. Kemmner, C. Gärtner, R. Klemm, K. S. Drese, and C. K. O'Sullivan, Lab Chip **11**, 625 (2011).
[181]C. Kellner, M. L. Botero, D. Latta, K. Drese, A. Fragoso, and C. K. O'Sullivan, Electrophoresis **32**, 926 (2011).
[182]R. Bruch, J. Baaske, C. Chatelle, M. Meirich, S. Madlener, W. Weber, C. Dincer, and G. A. Urban, Adv. Mater. **31**, 1905311 (2019).
[183]E. A. Phillips, T. J. Moehling, K. F. K. Ejendal, O. S. Hoilett, K. M. Byers, L. A. Basing, L. A. Jankowski, J. B. Bennett, L.-K. Lin, L. A. Stanciu, and J. C. Linnes, Lab Chip **19**, 3375 (2019).
[184]E. L. Fava, T. Martimiano do Prado, T. Almeida Silva, F. Cruz de Moraes, R. Censi Faria, and O. Fatibello-Filho, Electroanalysis. **32**, 1075 (2020).
[185]J. Yukird, V. Soum, O.-S. Kwon, K. Shin, O. Chailapakul, and N. Rodthongkum, Analyst **145**(4), 1491 (2020).
[186]R. M. Torrente-Rodríguez, H. Lukas, J. Tu, J. Min, Y. Yang, C. Xu, H. B. Rossiter, and W. Gao, Matter **3**, 1981 (2020).
[187]C. Liedert, L. Rannaste, A. Kokkonen, O.-H. Huttunen, R. Liedert, J. Hiltunen, and L. Hakalahti, ACS Sens. **5**, 2010 (2020).
[188]C. Duan, W. Wang, and Q. Xie, Biomicrofluidics **7**, 026501 (2013).
[189]G. Hu, J. Kang, L. W. T. Ng, X. Zhu, R. C. T. Howe, C. G. Jones, M. C. Hersam, and T. Hasan, Chem. Soc. Rev. **47**, 3265 (2018).
[190]W. Li, X. Xu, W. Li, P. Liu, Y. Zhao, Q. Cen, and M. Chen, J. Mater. Res. Technol. **9**, 142 (2020).
[191]C. Cano-Raya, Z. Z. Denchev, S. F. Cruz, and J. C. Viana, Appl. Mater. Today **15**, 416 (2019).
[192]M. Duta, M. Anastasescu, J. M. Calderon-Moreno, L. Predoana, S. Preda, M. Nicolescu, H. Stroescu, V. Bratan, I. Dascalu, E. Aperathitis, M. Modreanu, M. Zaharescu, and M. Gartner, J. Mater. Sci.: Mater. Electron. **27**, 4913 (2016).
[193]R. Schmidt, A. Basu, A. W. Brinkman, Z. Klusek, W. Kozlowski, S. Datta, A. Stiegelschmitt, and A. Roosen, Appl. Surf. Sci. **252**, 8760 (2006).
[194]M. N. Morshed, N. Behary, N. Bouazizi, J. Guan, G. Chen, and V. Nierstrasz, Sci. Rep. **9**, 15730 (2019).
[195]S. Ahuja, DMI Rev. **25**, 52 (2014).
[196]S. Reardon, New Sci. **219**, 20 (2013).
[197]J. T. Collins, J. Knapper, J. Stirling, J. Mduda, C. Mkindi, V. Mayagaya, G. A. Mwakajinga, P. T. Nyakyi, V. L. Sanga, D. Carbery, L. White, S. Dale, Z. Jieh Lim, J. J. Baumberg, P. Cicuta, S. McDermott, B. Vodenicharski, and R. Bowman, Biomed. Opt. Express **11**, 2447 (2020).
[198]J. S. Cybulski, J. Clements, and M. Prakash, PLoS One **9**, e98781 (2014).
[199]M. S. Bhamla, B. Benson, C. Chai, G. Katsikis, A. Johri, and M. Prakash, Nat. Biomed. Eng. **1**, 0009 (2017).
[200]E. A. Phillips, A. K. Young, N. Albarran, J. Butler, K. Lujan, K. Hamad-Schifferli, and J. Gomez-Marquez, Adv. Healthcare Mater. **7**, 1800104 (2018).
[201]C. E. Owens and A. J. Hart, Lab Chip **18**, 890 (2018).
[202]D. G. Rackus, I. H. Riedel-Kruse, and N. Pamme, Biomicrofluidics **13**, 041501 (2019).
[203]A. Chatmontree, S. Chairam, S. Supasorn, M. Amatatongchai, P. Jarujamrus, S. Tamuang, and E. Somsook, J. Chem. Educ. **92**, 1044 (2015).
[204]M. Levis, N. Kumar, E. Apakian, C. Moreno, U. Hernandez, A. Olivares, F. Ontiveros, and J. J. Zartman, Biomicrofluidics **13**, 024111 (2019).
[205]Z. Njus, T. Kong, U. Kalwa, C. Legner, M. Weinstein, S. Flanigan, J. Saldanha, and S. Pandey, APL Bioeng. **1**, 016102 (2017).
[206]A. L. Horst, J. M. Rosenbohm, N. Kolluri, J. Hardick, C. A. Gaydos, M. Cabodi, C. M. Klapperich, and J. C. Linnes, Biomed. Microdevices **20**, 35 (2018).
[207]B. L. Thompson, S. L. Wyckoff, D. M. Haverstick, and J. P. Landers, Anal. Chem. **89**, 3228 (2017).
[208]G. Xu, D. Nolder, J. Reboud, M. C. Oguike, D. A. van Schalkwyk, C. J. Sutherland, and J. M. Cooper, Angew. Chem., Int. Ed. **55**, 15250 (2016).
[209]T.-H. Kim, M. Lim, J. Park, J. M. Oh, H. Kim, H. Jeong, S. J. Lee, H. C. Park, S. Jung, B. C. Kim, K. Lee, M.-H. Kim, D. Y. Park, G. H. Kim, and Y.-K. Cho, Anal. Chem. **89**, 1155 (2017).
[210]I. Michael, D. Kim, O. Gulenko, S. Kumar, S. Kumar, J. Clara, D. Y. Ki, J. Park, H. Y. Jeong, T. S. Kim, S. Kwon, and Y.-K. Cho, Nat. Biomed. Eng. **4**, 591 (2020).
[211]J. Reboud, G. Xu, A. Garrett, M. Adriko, Z. Yang, E. M. Tukahebwa, C. Rowell, and J. M. Cooper, Proc. Natl. Acad. Sci. U.S.A. **116**, 4834 (2019).
[212]N. Bhalla, Y. Pan, Z. Yang, and A. F. Payam, ACS Nano **14**, 7783 (2020).
[213]M. N. Esbin, O. N. Whitney, S. Chong, A. Maurer, X. Darzacq, and R. Tjian, RNA **26**, 771 (2020).
[214]H. Zhao, F. Liu, W. Xie, T.-C. Zhou, J. OuYang, L. Jin, H. Li, C.-Y. Zhao, L. Zhang, J. Wei, Y.-P. Zhang, and C.-P. Li, Sens. Actuators, B **327**, 128899 (2021).
[215]J. U. Park, J. H. Lee, U. Paik, Y. Lu, and J. A. Rogers, Nano Lett. **8**, 4210 (2008).
[216]I. Rianasari, L. Walder, M. Burchardt, I. Zawisza, and G. Wittstock, Langmuir **24**, 9110 (2008).
[217]M. D. M. Dryden and A. R. Wheeler, PLoS One **10**, e0140349 (2015).
[218]O. S. Hoilett, J. F. Walker, B. M. Balash, N. J. Jaras, S. Boppana, and J. C. Linnes, Sensors **20**, 2407 (2020).
[219]Y. S. Zhang, J. Ribas, A. Nadhman, J. Aleman, Š Selimović, S. C. Lesher-Perez, T. Wang, V. Manoharan, S.-R. Shin, A. Damilano, N. Annabi, M. R. Dokmeci, S. Takayama, and A. Khademhosseini, Lab Chip **15**, 3661 (2015).
[220]I. Eydelnant, B. Betty Li, and A. Wheeler, "Microgels on-demand," Nat. Commun. **5**, 3355 (2014).